

## Chapter 3. Reconstructed Aerosol Light Extinction Coefficients

Light extinction in the atmosphere occurs when incident light is attenuated by the scattering and absorption of particles and gases in the layer through which it travels. The light extinction coefficient ( $b_{\text{ext}}$ ) is the fractional loss of intensity per unit path length. The Beer-Lambert law describes the intensity ( $F$ ) of an incident flux ( $F_0$ ) through a layer of thickness ( $z$ ) as

$$\frac{F}{F_0} = \exp(-b_{\text{ext}}z) \quad 3.1$$

The extinction coefficient can be written as the sum of scattering and absorption by particles ( $b_{\text{sp}}$  and  $b_{\text{ap}}$ , respectively) and gases ( $b_{\text{sg}}$  and  $b_{\text{ag}}$ , respectively) and has units of inverse length:

$$b_{\text{ext}} = b_{\text{sp}} + b_{\text{ap}} + b_{\text{sg}} + b_{\text{ag}} \quad 3.2$$

Absorption of light by gases is a well-understood phenomenon and straightforward to estimate. Visible light absorption is dominated by nitrogen dioxide ( $\text{NO}_2$ ) and can be estimated by multiplying  $\text{NO}_2$  concentrations by an absorption efficiency (Pitchford et al., 2007). Rayleigh scattering theory describes scattering of light by molecules ( $b_{\text{sg}}$ ) and depends on the density of the atmosphere. The highest values occur at sea level ( $\sim 12 \text{ Mm}^{-1}$ ), compared to the lowest levels at high elevations ( $8 \text{ Mm}^{-1}$  at  $\sim 3.5 \text{ km}$ ). Rayleigh scattering can vary due to temperature and pressure variations; it can be accurately determined if elevation and meteorological conditions are known.

Light extinction by particles is more complicated and depends strongly on particle size, composition, and hygroscopic properties. All particles scatter light and, if their size and refractive index are known, light scattering coefficients can be computed using Mie theory, assuming spherical particles. Light absorption by particles in the visible wavelengths is due to light absorbing carbon as well as some crustal mineral species. Because the required information necessary for performing Mie calculations is typically unknown (size distribution and concurrent aerosol composition measurements are time intensive and costly), the IMPROVE algorithm was developed to estimate aerosol light extinction coefficients. The algorithm assumes only speciated aerosol composition data are available (Malm et al., 1994).

### 3.1 IMPROVE AEROSOL LIGHT EXTINCTION COEFFICIENT ALGORITHM

Light extinction coefficients can be computed for an external mixture of aerosols by assuming a linear combination of species mass concentrations:

$$b_{\text{ext}} = \sum_j \alpha_j M_j \quad 3.3$$

The species ( $j$ ) mass concentration is given by  $M_j$  ( $\mu\text{g m}^{-3}$ ) and the extinction efficiency corresponding to that species is given by  $\alpha_j$  ( $\text{m}^2 \text{ g}^{-1}$ ). Equation 3.3 also holds for an internally mixed aerosol where the chemical species are mixed in fixed proportions to each other, the index of refraction is not a function of composition or size, and the aerosol density is independent of volume.

For hygroscopic species (species that absorb water), the linear relationship between light extinction coefficients and mass shown in equation 3.3 will not hold because of the nonlinear behavior of particle growth and  $b_{\text{ext}}$  with increased relative humidity (RH). To account for this effect, the extinction efficiencies are multiplied by a humidification factor ( $f(\text{RH}) = b_{\text{sp,RH}}/b_{\text{sp,dry}}$ ) that is a ratio of humidified ( $b_{\text{sp,RH}}$ ) to dry ( $b_{\text{sp,dry}}$ ) light scattering coefficients that accounts for the effects of changing RH on extinction coefficients. Humidification factors are computed by assuming a size distribution and composition-dependent growth factor (e.g., Hand et al., 2010).

The original IMPROVE equation has been used extensively to reconstruct  $b_{\text{ext}}$ , using measured aerosol composition (e.g., Malm et al., 1994; Lowenthal and Kumar, 2003; Malm et al., 2005; Malm and Hand, 2007; Brewer and Moore, 2009), and was adopted by the Environmental Protection Agency (EPA) as a metric for tracking progress in reducing haze levels under the 1999 Regional Haze Rule (RHR) (Pitchford et al., 2007). In 2005 a review was initiated by the IMPROVE steering committee to investigate possible biases in light extinction coefficients as computed by the algorithm (Hand and Malm, 2006; Malm and Hand, 2007). The review resulted in the revised IMPROVE algorithm that is now being used by most states in their state implementation plans (Pitchford et al., 2007). Discussions of the RHR and results using the revised IMPROVE equation are presented in Chapter 9.

The algorithm applied in this report is a combination of the original and revised algorithms and will be referred to here as the “modified original” algorithm. The original algorithm included contributions from ammonium sulfate, ammonium nitrate, particulate organic matter, light absorbing carbon, soil, and coarse mass and a constant Rayleigh scattering term. The modified original algorithm differs from the original in that it included several changes deemed important during the 2005 review. Specifically, sea salt was included and a factor of 1.8 was applied to compute particulate organic matter from organic carbon concentrations. Site-specific Rayleigh scattering was also included, rather than the constant value of  $10 \text{ Mm}^{-1}$  assumed in the original equation. The modified original algorithm differs from the revised algorithm in that it applies constant mass extinction efficiencies for each species. Mean  $b_{\text{ext}}$  computed by the modified original algorithm should not differ significantly from  $b_{\text{ext}}$  computed with the revised algorithm. The modified original algorithm is presented in equation 3.4:

$$b_{\text{ext}} = 3f(\text{RH})[\text{ammonium sulfate}] + 3f(\text{RH})[\text{ammonium nitrate}] + 4[\text{particulate organic matter}] + 10[\text{light absorbing carbon}] + 1[\text{soil}] + 1.7f(\text{RH})_{\text{ss}}[\text{sea salt}] + 0.6[\text{coarse mass}] + \text{site-specific Rayleigh scattering} \quad 3.4$$

The units of  $b_{\text{ext}}$  and Rayleigh scattering are in inverse megameters ( $\text{Mm}^{-1}$ ). Mass concentrations of aerosol species are in  $\mu\text{g m}^{-3}$ , and mass scattering and absorption efficiencies have units of  $\text{m}^2 \text{g}^{-1}$ . Dry mass scattering and absorption efficiencies were rounded to one significant digit to represent the degree of uncertainty associated with these values. Values of  $3 \text{ m}^2 \text{g}^{-1}$  were used for both ammonium sulfate and ammonium nitrate,  $4 \text{ m}^2 \text{g}^{-1}$  for particulate organic matter,  $10 \text{ m}^2 \text{g}^{-1}$  for light absorbing carbon,  $1 \text{ m}^2 \text{g}^{-1}$  for soil,  $1.7 \text{ m}^2 \text{g}^{-1}$  for sea salt, and  $0.6 \text{ m}^2 \text{g}^{-1}$  for coarse mass. These values correspond to a wavelength of 550 nm (Hand and Malm, 2007). Comparisons of  $b_{\text{ext}}$  for IMPROVE and the CSN are limited to  $\text{PM}_{2.5}$  aerosol  $b_{\text{ext}}$  because coarse mass is not measured as part of the CSN.

Daily  $b_{\text{ext}}$  values were computed using equation 3.4; monthly mean values were computed from daily  $b_{\text{ext}}$ . Daily  $b_{\text{ext}}$  values that were less than zero were treated as missing data. This treatment was different than the mass concentration analyses that allowed for negative mass values for some species (e.g., blank-corrected ion concentrations could be negative). Therefore, some differences between patterns in mass and  $b_{\text{ext}}$  values may be due to this difference, most notably for nonhygroscopic species where  $b_{\text{ext}}$  values are just scaled mass concentrations.

The  $f(\text{RH})$  values applied in equation 3.4 were computed using the algorithm outlined in the Regional Haze Rule Guidelines for Tracking Progress (U.S. EPA, 2003) and were the same values applied in previous IMPROVE reports. A lognormal ammonium sulfate mass size distribution with a geometric mass mean diameter of  $0.3 \mu\text{m}$  and a geometric standard deviation of 2.0 was used with Mie theory to compute  $f(\text{RH})$ . An interpolation between the deliquescence and efflorescence curves was performed to obtain a smoothed  $f(\text{RH})$  curve. This same curve was applied to ammonium nitrate. The  $f(\text{RH})_{\text{ss}}$  applied to sea salt was computed assuming a sea salt geometric mass mean diameter of  $2.5 \mu\text{m}$  and a geometric standard deviation of 2 (Pitchford et al., 2007). We assumed that POM was nonhygroscopic. Figure 3.1 presents the  $f(\text{RH})$  curve applied to ammonium sulfate and ammonium nitrate in equation 3.4. Humidification factors are unitless.

Monthly and site-specific  $f(\text{RH})$  curves were generated based on monthly climatological mean RH values. These monthly RH values eliminate the effects of interannual variations in RH while maintaining typical regional and seasonal humidity patterns around the United States. The EPA produced recommended monthly  $f(\text{RH})$  values for each Class I area, based on analysis of a 10-year record (1988–1997) of hourly RH data from 292 National Weather Service stations across the 50 states and the District of Columbia, as well as from 29 IMPROVE and IMPROVE protocol monitoring sites, 48 Clean Air Status and Trends Network (CASTNet) sites, and 13 additional sites administered by the National Park Service. Values of  $f(\text{RH})$  for other IMPROVE sites (non-Class I area sites) were generated using an interpolation scheme with an inverse distance weighting technique (U.S. EPA, 2001). The daily humidified ammonium sulfate and ammonium nitrate and sea salt extinction coefficients for each site were calculated using this lookup table. Values of  $f(\text{RH})$  varied significantly depending on time of year and site location. For example, the  $f(\text{RH})$  value in Douglas, Arizona (DOUG1), in August was 1.84, compared to 3.88 in Linville Gorge, North Carolina (LIGO1). In April, the  $f(\text{RH})$  at DOUG1 was 1.16, compared to 2.65 at LIGO1. For a constant ammonium sulfate mass, its light scattering coefficient can double based only on hygroscopic effects. Estimates of  $f(\text{RH})$  for CSN sites were determined similarly to IMPROVE sites by using a lookup table with site locations.

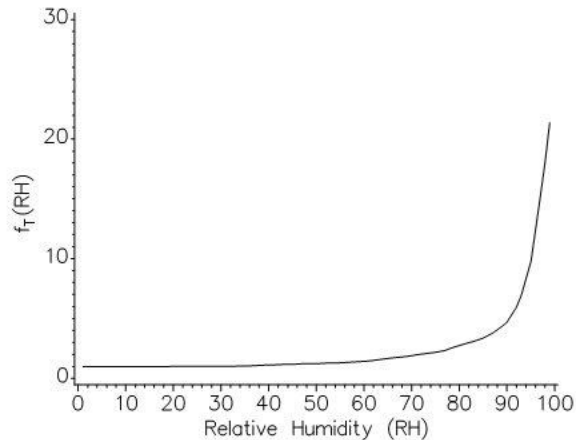


**Figure 3.1. Humidification factor ( $f_T(RH)$ ) as a function of relative humidity (RH) A lognormal ammonium sulfate mass size distribution with a geometric mass mean diameter of  $0.3 \mu\text{m}$  and a geometric standard deviation of 2.0 was assumed. A wavelength of 550 nm was used.**

Visual range and extinction measurements are nonlinear with respect to human perception of visual scene changes caused by haze. The deciview haze index ( $dv$ ) was derived with a number of assumptions such that uniform changes in haze correspond to approximately uniform incremental changes in visual perception (Pitchford and Malm, 1994). Deciview was calculated from reconstructed  $b_{ext}$ , using equation 3.5:

$$dv = 10\ln(b_{ext}/10) \tag{3.5}$$

Deciview corresponds to the total  $b_{ext}$ , including the contribution of coarse mass. Because of the absence of coarse mass from the CSN network,  $dv$  was computed using only IMPROVE data. In the original IMPROVE equation,  $dv = 0$  for pristine (near-Rayleigh scattering) conditions (elevations  $\sim 1.8$  km). Now that site-specific Rayleigh scattering is included in equation 3.5 in the place of  $10 \text{ Mm}^{-1}$ , it is actually possible to have a negative  $dv$  for pristine conditions at sites with very low Rayleigh scattering ( $\sim 3.5$  km).

In the following sections we present spatial patterns of 2005–2008 annual mean reconstructed  $b_{ext}$  corresponding to ammonium sulfate, ammonium nitrate, particulate organic matter, light absorbing carbon, soil, sea salt, aerosol, coarse mass (IMPROVE only), and deciview (IMPROVE only) for IMPROVE and CSN sites. For many species (those that were considered nonhygroscopic) the  $b_{ext}$  maps were similar to the mass concentration maps, but scaled by extinction efficiencies. Percent contributions of each species to  $\text{PM}_{2.5}$  aerosol  $b_{ext}$  are also presented. As with the mass concentration maps, caution should be taken to avoid over-interpreting these maps as they are interpolations of irregularly gridded data and are provided only to reflect general spatial patterns. The top number in the scale of each contour map corresponds to the maximum  $b_{ext}$  for all sites, although the contours themselves were created with the highest level set to the 95<sup>th</sup> percentile in  $b_{ext}$ .

### 3.2 PM<sub>2.5</sub> AMMONIUM SULFATE LIGHT EXTINCTION COEFFICIENTS

The 2005–2008 annual mean light extinction coefficients corresponding to ammonium sulfate ( $b_{\text{ext\_AS}}$ ) ranged from 2.88  $\text{Mm}^{-1}$  in Sawtooth National Forest (NF), Idaho (SAWT1), to 65.24  $\text{Mm}^{-1}$  in Mammoth Cave, Kentucky (MACA1), for rural IMPROVE sites (Figure 3.2a). The maximum  $b_{\text{ext\_AS}}$  for urban IMPROVE sites was comparable (59.83  $\text{Mm}^{-1}$  in Birmingham, Alabama, BIRM1). The minimum IMPROVE urban  $b_{\text{ext\_AS}}$  (5.96  $\text{Mm}^{-1}$ , Phoenix, Arizona, PHOE5) was somewhat higher than the rural minimum. Light extinction coefficients from ammonium sulfate were much higher in the eastern United States compared to the western United States. The same east-west division observed for the annual mean ammonium sulfate mass concentrations was observed for  $b_{\text{ext}}$ , but  $b_{\text{ext}}$  was more “focused” spatially due to relative humidity effects in the eastern United States. Sites along the Ohio River valley and Appalachian Mountains corresponded to the highest  $b_{\text{ext\_AS}}$ . The magnitude of  $b_{\text{ext\_AS}}$  was comparable to the contribution from Rayleigh scattering (10–12  $\text{Mm}^{-1}$ ) for 54–60% of all IMPROVE sites, and the majority of these were located in the western United States. The addition of CSN sites did not alter the spatial pattern of  $b_{\text{ext\_AS}}$  significantly, except in Texas and Louisiana, where the addition of sites provided additional spatial detail (Figure 3.2b). The maximum  $b_{\text{ext\_AS}}$  for the CSN network occurred in Liberty, Pennsylvania (74.64  $\text{Mm}^{-1}$ , #420030064), compared to the lowest  $b_{\text{ext\_AS}}$  in Reno, Nevada (4.66  $\text{Mm}^{-1}$ , #320310016). The similarity in the spatial patterns and magnitudes of  $b_{\text{ext\_AS}}$  for the rural and urban sites suggested regional sources of ammonium sulfate and meteorological conditions that contribute to high  $b_{\text{ext\_AS}}$  on regional scales.

In the eastern United States, the IMPROVE aerosol  $b_{\text{ext}}$  was dominated by ammonium sulfate, with percent contributions to  $b_{\text{ext}}$  greater than 50% (Figure 3.2c). Overall, ammonium sulfate was a significant contributor to aerosol  $b_{\text{ext}}$ , with 96% of all IMPROVE sites corresponding to a contribution to aerosol  $b_{\text{ext}}$  of greater than 20%. The site with the highest contribution of ammonium sulfate to  $b_{\text{ext}}$  was Hawaii Volcanoes (HAVO1, 86.6%), compared to the minimum at Sawtooth NF, Idaho (15.7%, SAWT1). The IMPROVE urban contribution to  $b_{\text{ext}}$  from ammonium sulfate ranged from 11.9% (Fresno, California, FRES1) to 58.5% (Baltimore, Maryland, BALT1). The percent contribution of ammonium sulfate to  $b_{\text{ext}}$  at the CSN sites ranged from 9.5% (Reno, #320310016) to 75.1% (Charleston, West Virginia, #540390011), with very similar spatial patterns as the rural network (Figure 3.2d). However, in general urban aerosol  $b_{\text{ext}}$  was not as dominated by ammonium sulfate as compared to the rural network. Only 88% of CSN sites corresponded to contributions of ammonium sulfate to  $b_{\text{ext}}$  of greater than 20%, even though most of the CSN sites are in the eastern United States, where  $b_{\text{ext\_AS}}$  values were the highest.

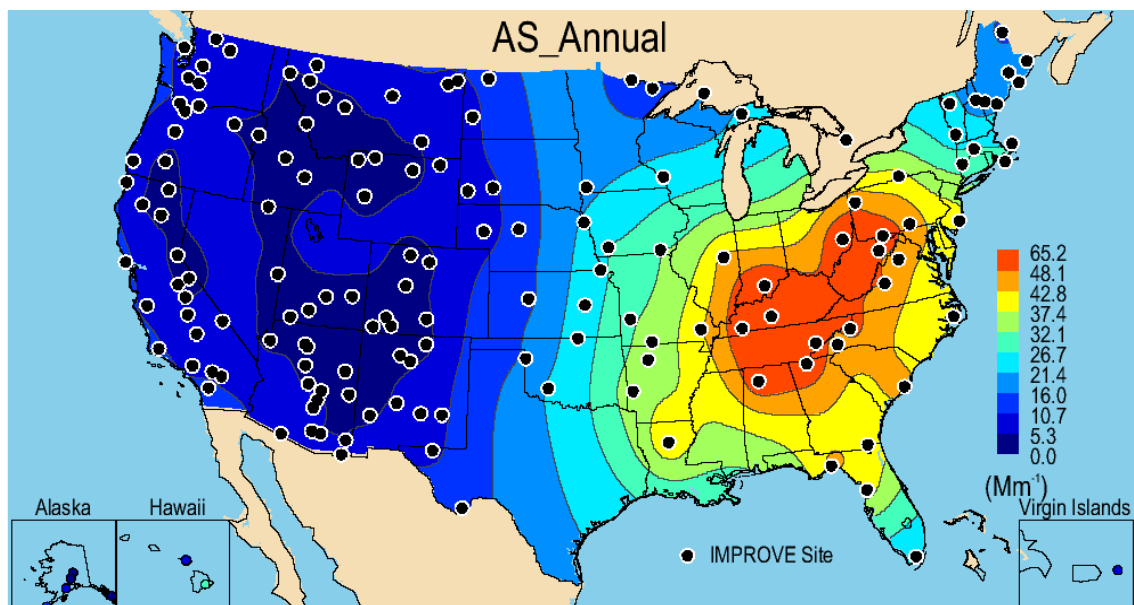


Figure 3.2a.  $PM_{2.5}$  reconstructed ambient annual mean light extinction coefficient for ammonium sulfate ( $b_{ext\_AS}$ ,  $Mm^{-1}$ ) for 2005–2008 for rural IMPROVE sites. The “modified original” IMPROVE algorithm was used (see text). Wavelength corresponds to 550 nm.

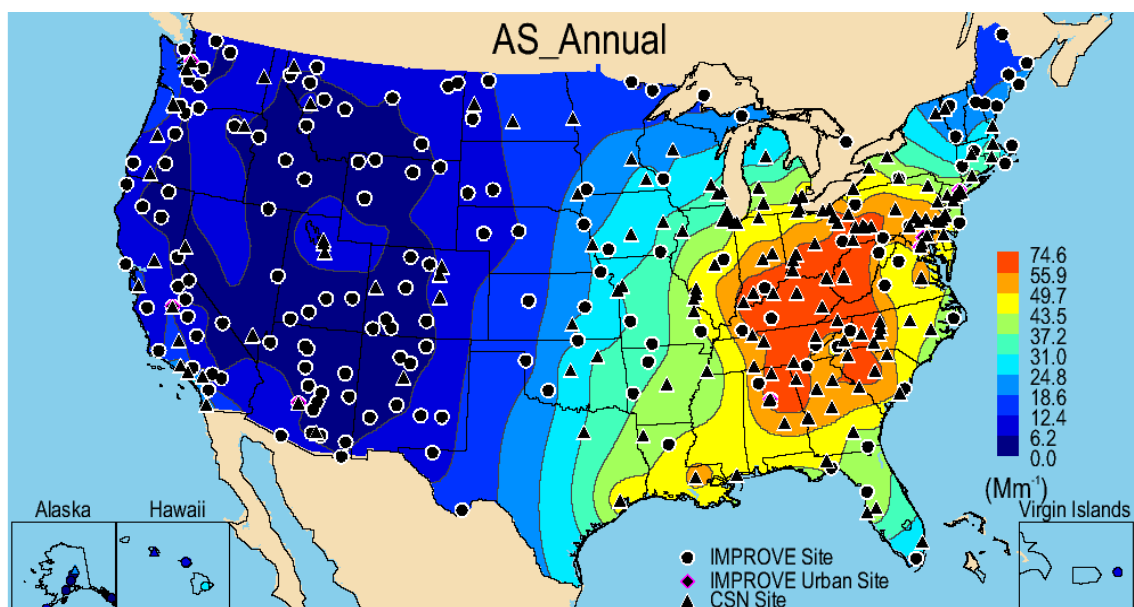


Figure 3.2b.  $PM_{2.5}$  reconstructed ambient annual mean light extinction coefficient for ammonium sulfate ( $b_{ext\_AS}$ ,  $Mm^{-1}$ ) for 2005–2008 for rural IMPROVE and urban CSN sites. The “modified original” IMPROVE algorithm was used (see text). Wavelength corresponds to 550 nm.

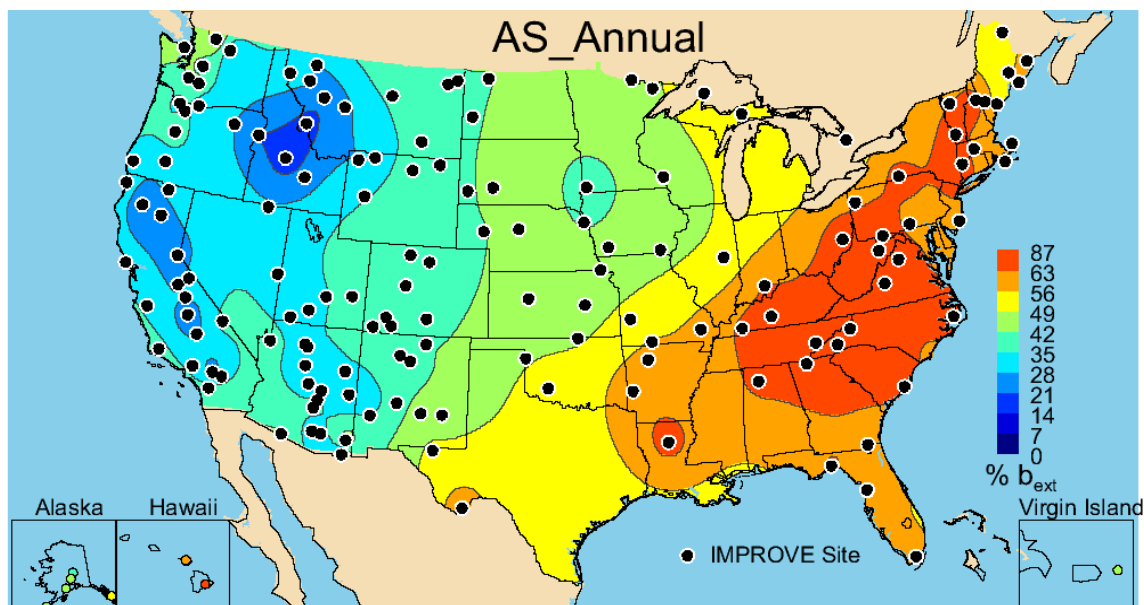


Figure 3.2c. Annual mean percent contribution (%) of ambient ammonium sulfate (AS) light extinction coefficient ( $b_{ext}$ ) to  $PM_{2.5}$  reconstructed aerosol  $b_{ext}$  for 2005–2008 for rural IMPROVE sites. The “modified original” IMPROVE algorithm was used (see text). Wavelength corresponds to 550 nm.

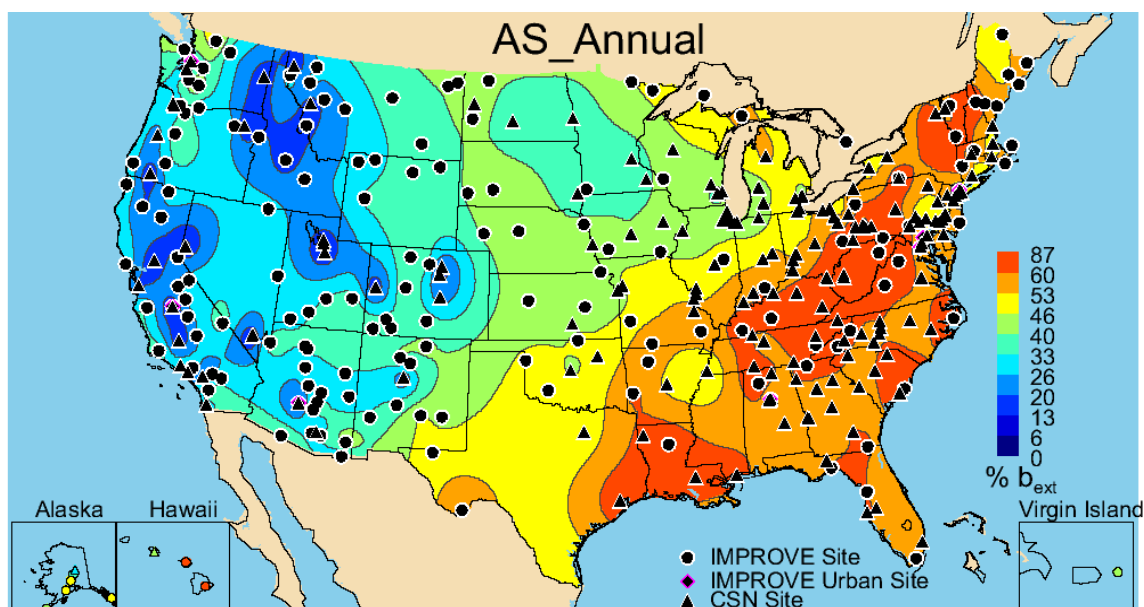


Figure 3.2d. Annual mean percent contribution (%) of ambient ammonium sulfate (AS) light extinction coefficient ( $b_{ext}$ ) to  $PM_{2.5}$  reconstructed aerosol  $b_{ext}$  for 2005–2008 for rural IMPROVE and urban CSN sites. The “modified original” IMPROVE algorithm was used (see text). Wavelength corresponds to 550 nm.

### 3.3 $PM_{2.5}$ AMMONIUM NITRATE LIGHT EXTINCTION COEFFICIENTS

The spatial pattern of the 2005–2008 rural IMPROVE annual mean ammonium nitrate light extinction coefficient ( $b_{ext\_AN}$ ) was nearly identical to the annual mean mass concentration pattern (Figure 3.3a). Regions of elevated  $b_{ext\_AN}$  were located in the central United States and on the West Coast. Rural IMPROVE estimates ranged from  $0.47 \text{ Mm}^{-1}$  in Petersburg, Alaska (PETE1), to  $27.87 \text{ Mm}^{-1}$  in Bondville, Illinois (BOND1), located in the agricultural Midwest. In

general, however, most of the rural sites corresponded to low ( $< 10 \text{ Mm}^{-1}$ )  $b_{\text{ext\_AN}}$ . Not surprisingly, urban IMPROVE sites corresponded to higher  $b_{\text{ext\_AN}}$  ( $5.68 \text{ Mm}^{-1}$ ) in Phoenix (PHOE5), to  $53.27 \text{ Mm}^{-1}$  in Fresno (FRES1). Several urban CSN sites also corresponded to high  $b_{\text{ext\_AN}}$ , including sites in the western United States such as Rubidoux, California (with the highest  $b_{\text{ext\_AN}}$  of  $60.49 \text{ Mm}^{-1}$ , #060658001), San Francisco, Sacramento, Salt Lake City, and Denver (Figure 3.3b). The central and Midwest sites with high urban  $b_{\text{ext\_AN}}$  stretched eastward, with the inclusion of several sites in Indiana, Michigan, and Ohio. In general the urban sites had higher  $b_{\text{ext\_AN}}$ ; only 24% of CSN sites corresponded to  $b_{\text{ext\_AN}}$  less than  $10 \text{ Mm}^{-1}$ , and 50% of CSN sites had annual  $b_{\text{ext\_AN}}$  greater than  $15 \text{ Mm}^{-1}$ . The lowest annual mean CSN  $b_{\text{ext\_AN}}$  occurred in Honolulu ( $1.82 \text{ Mm}^{-1}$ , #150032004).

The spatial pattern of the percent contribution of ammonium nitrate to  $b_{\text{ext}}$  somewhat mirrored the  $b_{\text{ext\_AN}}$  pattern (see Figure 3.3c), except in the Northwest and in California. Although sites in these regions did not correspond to the highest ammonium nitrate mass concentrations, they do correspond to significant contributions of AN to  $b_{\text{ext}}$ . Also, in the Midwest ammonium nitrate was a significant contributor to  $b_{\text{ext}}$  at many sites; at 21% of IMPROVE sites, ammonium nitrate contributed over 20% to  $b_{\text{ext}}$ . In the northern Great Plains, the annual mean percent contribution to  $b_{\text{ext}}$  was 27.8% at Lostwood, North Dakota (LOST1), 25.7% at Medicine Lake, Montana (MELA1), and 24.9% at Fort Peck, Montana (FOPE1). The highest contribution to the annual mean  $b_{\text{ext}}$  occurred at Blue Mounds, Minnesota (40.5%), compared to the lowest percent contribution at Hawaii Volcanoes (2.4%, HAVO1). The largest percent contribution to  $b_{\text{ext}}$  at an urban IMPROVE site occurred at Fresno (FRES1) where 49.3% of the  $b_{\text{ext}}$  was due to ammonium nitrate. The lowest urban IMPROVE percent contribution occurred at Birmingham, Alabama (8.5%, BIRM1). AN contributed significantly to  $b_{\text{ext}}$  at CSN sites. At slightly more than half (52%) of all CSN sites, ammonium nitrate contributed over 20% to annual  $b_{\text{ext}}$  (Figure 3.3d). The impact of urban AN percent contribution to  $b_{\text{ext}}$  was obvious from the inclusion of those sites in the interpolation. Sites in Utah, Colorado, and California all corresponded to high percent contributions to  $b_{\text{ext}}$ , as well as additional sites in the central United States (Indiana, Michigan, and Ohio). The highest percent contribution to  $b_{\text{ext}}$  occurred in Bakersfield, California (53.9%, #060290014), compared to the lowest in Douglas, Georgia (6.3%, #130690002).

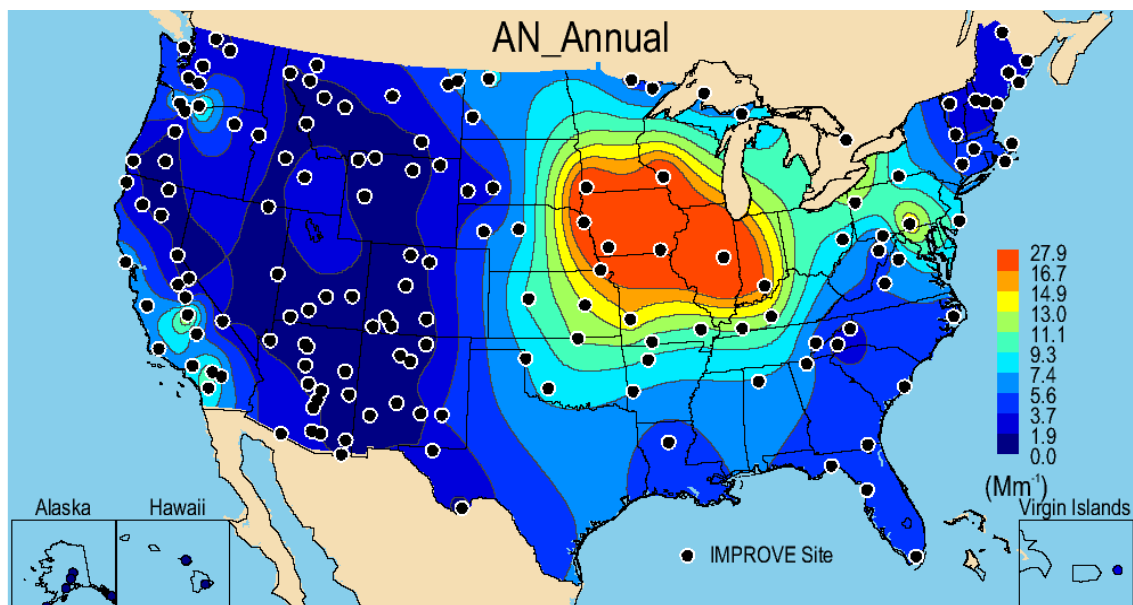


Figure 3.3a.  $\text{PM}_{2.5}$  reconstructed ambient annual mean light extinction coefficient for ammonium nitrate ( $b_{\text{ext\_AN}}$ ,  $\text{Mm}^{-1}$ ) for 2005–2008 for rural IMPROVE sites. The “modified original” IMPROVE algorithm was used (see text). Wavelength corresponds to 550 nm.

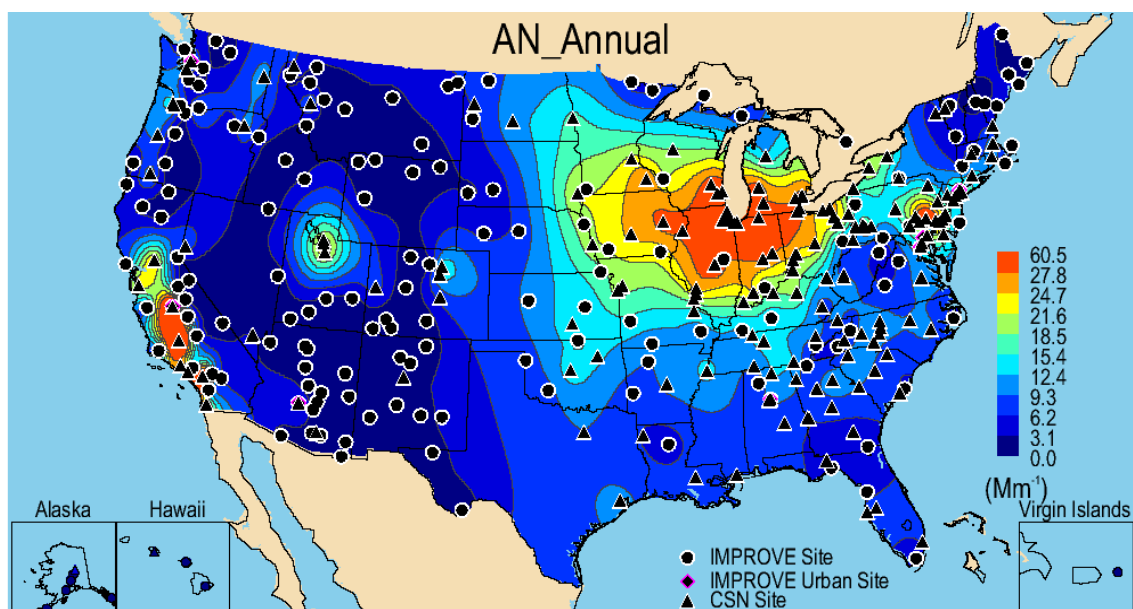


Figure 3.3b.  $\text{PM}_{2.5}$  reconstructed ambient annual mean light extinction coefficient for ammonium nitrate ( $b_{\text{ext\_AN}}$ ,  $\text{Mm}^{-1}$ ) for 2005–2008 for rural IMPROVE and urban CSN sites. The “modified original” IMPROVE algorithm was used (see text). Wavelength corresponds to 550 nm.

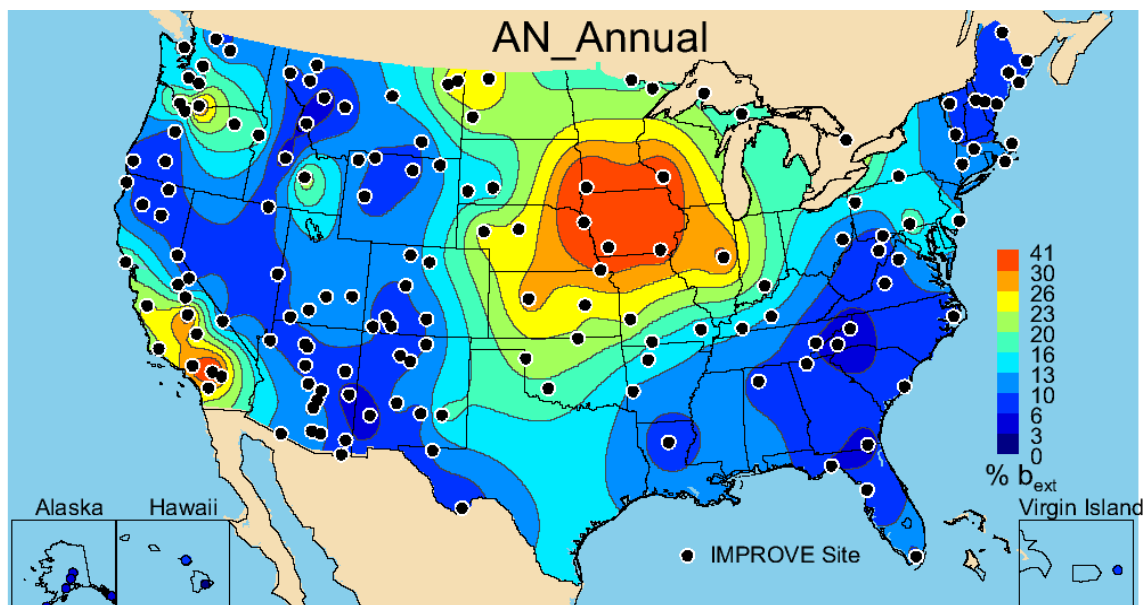


Figure 3.3c. Annual mean percent contribution (%) of ambient ammonium nitrate (AN) light extinction coefficient ( $b_{ext}$ ) to  $PM_{2.5}$  reconstructed aerosol  $b_{ext}$  for 2005–2008 for rural IMPROVE sites. The “modified original” IMPROVE algorithm was used (see text). Wavelength corresponds to 550 nm.

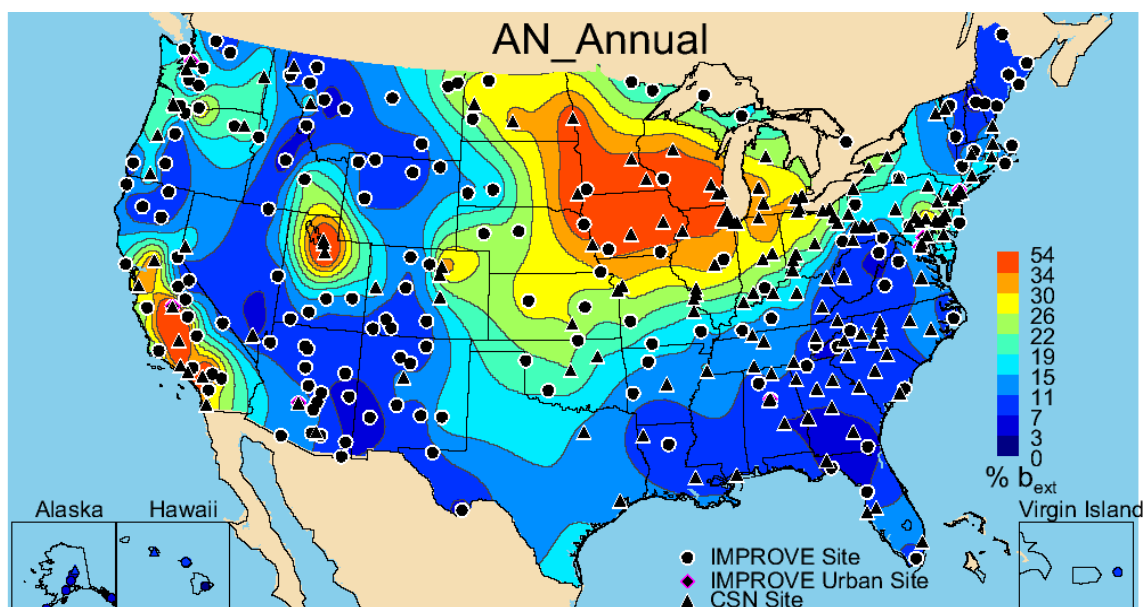


Figure 3.3d. Annual mean percent contribution (%) of ambient ammonium nitrate (AN) light extinction coefficient ( $b_{ext}$ ) to  $PM_{2.5}$  reconstructed aerosol  $b_{ext}$  for 2005–2008 for rural IMPROVE and urban CSN sites. The “modified original” IMPROVE algorithm was used (see text). Wavelength corresponds to 550 nm.

### 3.4 $PM_{2.5}$ PARTICULATE ORGANIC MATTER LIGHT EXTINCTION COEFFICIENTS

The 2005–2008 IMPROVE annual mean light extinction coefficient due to particulate organic matter ( $b_{ext\_POM}$ ) ranged from  $1.08 \text{ Mm}^{-1}$  (Virgin Islands, VIIS1) to  $18.25 \text{ Mm}^{-1}$  in Trinity, California (TRIN1), for rural IMPROVE sites, and  $14.34 \text{ Mm}^{-1}$  (Puget Sound, Washington, PUSO1) to  $27.93 \text{ Mm}^{-1}$  (Birmingham, BIRM1) for urban IMPROVE sites. POM

was considered nonhygroscopic in the algorithm for computing  $b_{\text{ext}}$ , so the spatial pattern of  $b_{\text{ext\_POM}}$  reflected that of the POM annual mean mass concentration pattern (Figure 3.4a). High levels of  $b_{\text{ext\_POM}}$  were observed in the southern and southeastern United States and in urban regions in the Southwest (Phoenix) and California (Fresno). Other regions with high levels of  $b_{\text{ext\_POM}}$  were observed in northern California and in Idaho and Montana, most likely due to emissions from wildfires. For most sites, however,  $b_{\text{ext\_POM}}$  was fairly low, which included most sites in the Midwest and western states. The  $b_{\text{ext\_POM}}$  was higher for urban CSN sites, similar to urban POM mass concentrations (Figure 3.4b). Values ranged from  $6.69 \text{ Mm}^{-1}$  (Fargo, North Dakota, #380171004) to  $46.86 \text{ Mm}^{-1}$  in Libby, Montana (#300530018). In contrast to the rural sites, most of the urban sites had  $b_{\text{ext\_POM}}$  greater than  $10 \text{ Mm}^{-1}$ . With the inclusion of urban site data in the interpolation, higher gradients surrounding cities were observed, suggesting local urban sources of organic aerosols. Regional sources (perhaps biogenic or wildfire emissions) seemed more spatially extensive in the Southeast compared to more localized sources for many urban centers in the West. In general, urban  $b_{\text{ext\_POM}}$  was higher than rural  $b_{\text{ext\_POM}}$ .

The rural IMPROVE percent contribution of POM to aerosol  $b_{\text{ext}}$  is presented in Figure 3.4c. The east-west divide seen in many spatial maps was also observed here but in reverse. Percent contributions of  $b_{\text{ext\_POM}}$  were higher in the West, typically greater than 30%. Regions in northern California, Oregon, Idaho, Montana, and Wyoming were the highest, most likely due to the role of wildfire emissions and relatively low emissions from other major contributors to  $b_{\text{ext}}$ . Forty-one percent of all IMPROVE sites corresponded to contributions over 30% to  $b_{\text{ext}}$ , probably due to the density of IMPROVE sites in the West. The maximum percent contribution occurred at Sawtooth, Idaho (70.2%, SAWT1), compared to the lowest at Hawaii Volcano (3.3%, HAVO1). At IMPROVE urban sites the percent contribution ranged from 15.8% (Baltimore, BALT1) to 42.3% (Phoenix, PHOE1). A similar pattern was observed with the addition of the CSN sites, with higher percent contributions in the West (Figure 3.4d). Interestingly, sites in Utah corresponded to lower percent contributions compared to surrounding areas, likely because of the contribution from ammonium nitrate to  $b_{\text{ext}}$  (see Figure 3.3d) at these sites. The percent contribution ranged from 10.14% (Indianapolis, #180650003) to 66.10% in Libby, Montana (#300530018). Only 10% of CSN sites corresponded to a percent contribution greater than 30%, reflecting the high density of sites in the East where ammonium sulfate is the main contributor to  $b_{\text{ext}}$ .

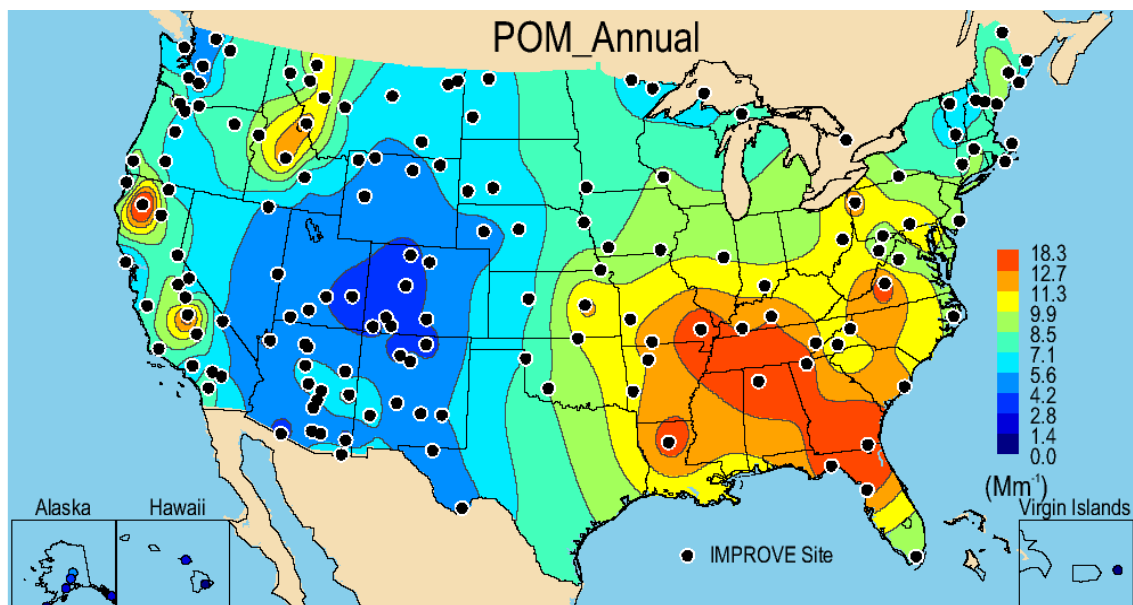


Figure 3.4a.  $PM_{2.5}$  reconstructed ambient annual mean light extinction coefficient for particulate organic matter (POM) ( $b_{ext\_POM}$ ,  $Mm^{-1}$ ) for 2005–2008 for rural IMPROVE sites. The “modified original” IMPROVE algorithm was used (see text). Wavelength corresponds to 550 nm.

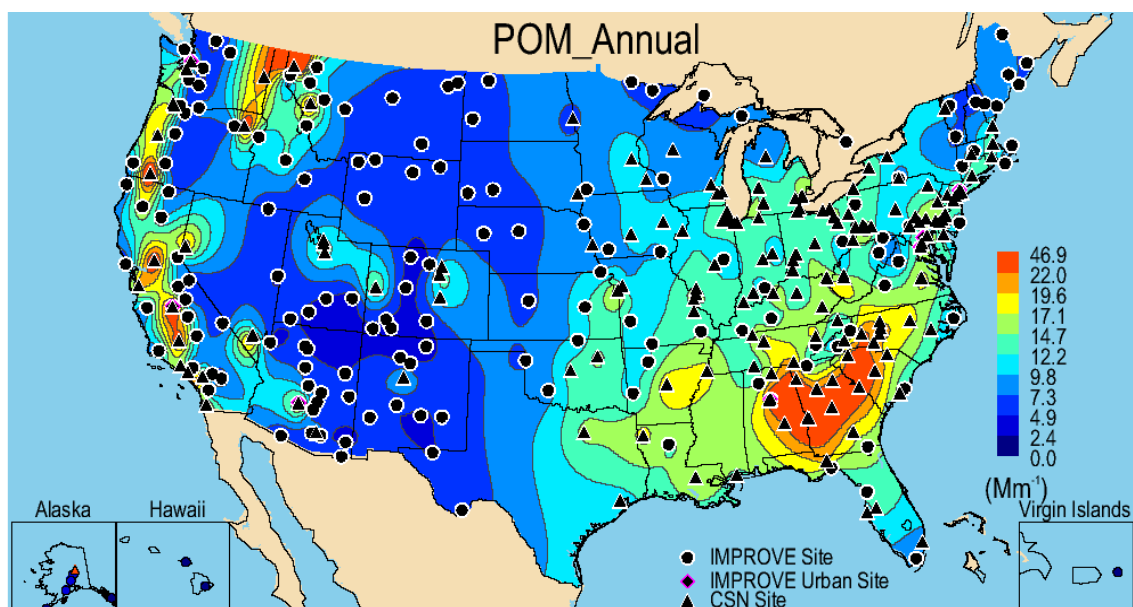


Figure 3.4b.  $PM_{2.5}$  reconstructed ambient annual mean light extinction coefficient for particulate organic matter (POM) ( $b_{ext\_POM}$ ,  $Mm^{-1}$ ) for 2005–2008 for rural IMPROVE and urban CSN sites. The “modified original” IMPROVE algorithm was used (see text). Wavelength corresponds to 550 nm.

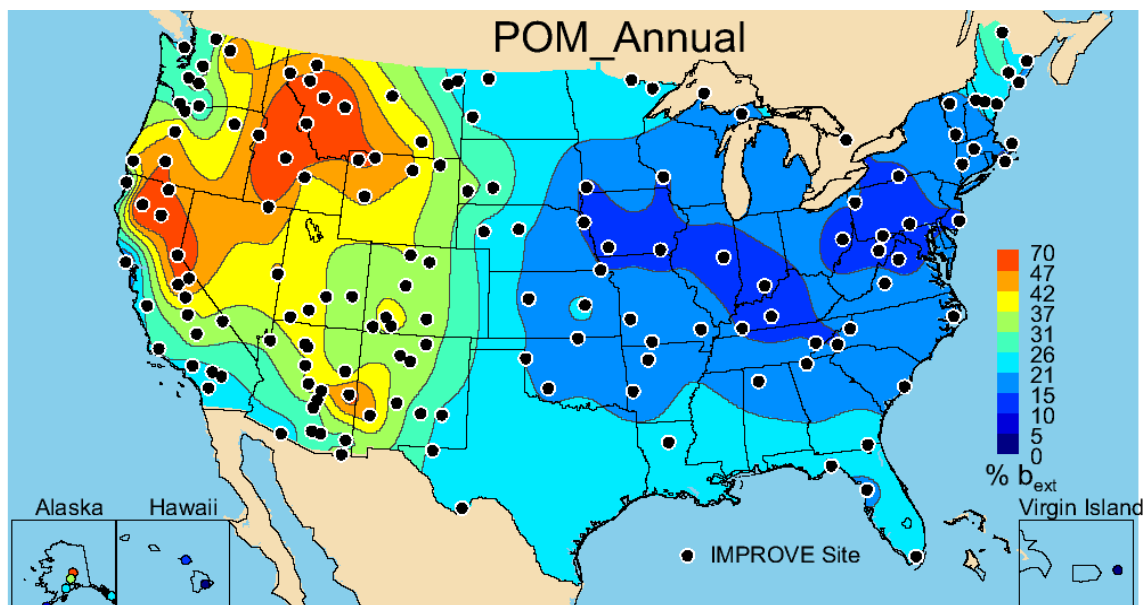


Figure 3.4c. Annual mean percent contribution (%) of ambient particulate organic matter (POM) light extinction coefficient ( $b_{ext}$ ) to  $PM_{2.5}$  reconstructed aerosol  $b_{ext}$  for 2005–2008 for rural IMPROVE sites. The “modified original” IMPROVE algorithm was used (see text). Wavelength corresponds to 550 nm.

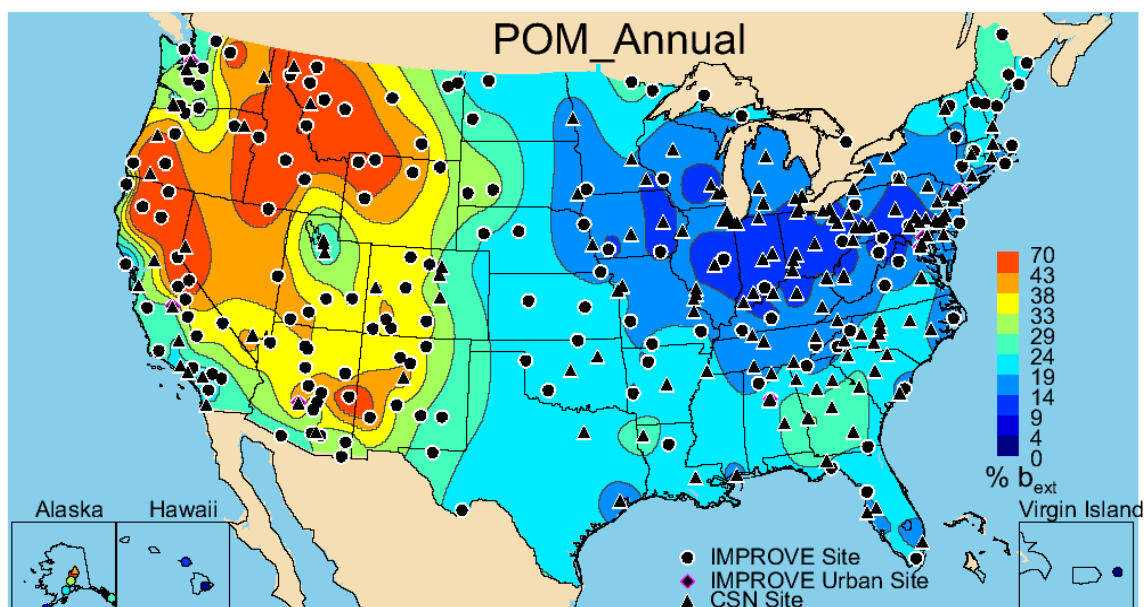


Figure 3.4d. Annual mean percent contribution (%) of ambient particulate organic matter (POM) light extinction coefficient ( $b_{ext}$ ) to  $PM_{2.5}$  reconstructed aerosol  $b_{ext}$  for 2005–2008 for rural IMPROVE and urban CSN sites. The “modified original” IMPROVE algorithm was used (see text). Wavelength corresponds to 550 nm.

### 3.5 $PM_{2.5}$ LIGHT ABSORBING CARBON LIGHT EXTINCTION COEFFICIENTS

The IMPROVE spatial pattern of 2005–2008 annual mean extinction coefficients from light absorbing carbon ( $b_{ext\_LAC}$ ) were similar to the LAC mass concentration patterns, with elevated levels at eastern sites (Figure 3.5a). The maximum annual mean rural  $b_{ext\_LAC}$  ( $5.91 \text{ Mm}^{-1}$ ) occurred at James River Face Wilderness (JARI1) in Virginia, similar to the high

LAC mass concentration. The lowest rural  $b_{\text{ext\_LAC}}$  occurred at Hawaii Volcano ( $0.36 \text{ Mm}^{-1}$ , HAVO1). Most (93%) IMPROVE sites corresponded to very low ( $< 5 \text{ Mm}^{-1}$ )  $b_{\text{ext\_LAC}}$ . The only IMPROVE sites with higher annual mean  $b_{\text{ext\_LAC}}$  corresponded to urban sites as seen in Figure 3.5b. The addition of CSN sites extended the localized impact of LAC on  $b_{\text{ext}}$  to a number of other sites in major urban centers. Strong gradients surrounding these sites suggested local sources with fairly localized effects on visibility. The minimum urban  $b_{\text{ext\_LAC}}$  was greater than at the maximum rural site ( $8.50 \text{ Mm}^{-1}$  at Puget Sound, PUSO1), and the maximum urban IMPROVE  $b_{\text{ext\_LAC}}$  occurred at Birmingham ( $16.56 \text{ Mm}^{-1}$ , BIRM1). The CSN estimates ranged from  $1.34 \text{ Mm}^{-1}$  in Watford City, North Dakota (#380530002) to  $25.81 \text{ Mm}^{-1}$  in Liberty (#420030064). In contrast to the rural sites, only 13% of urban sites corresponded to  $b_{\text{ext\_LAC}}$  less than  $5 \text{ Mm}^{-1}$ , suggesting the importance of urban sources of LAC to  $b_{\text{ext}}$  at urban sites.

Although rural  $b_{\text{ext\_LAC}}$  was higher in the East, its percent contribution to  $b_{\text{ext}}$  was higher in the West (Figure 3.5c). Biomass combustion sources (wildfire and wood burning) in the West were relatively more important, as suggested by the higher percent contribution in the northwestern United States. Rural percent contributions ranged from 1.1% (Hawaii Volcano, HAVO1) to 16.7% in Petrified Forest, Arizona (PEFO1). IMPROVE urban sites in the Southwest also corresponded to higher percent contributions of LAC to  $b_{\text{ext}}$ . In urban IMPROVE regions,  $b_{\text{ext\_LAC}}$  ranged from 9.4% (Baltimore, BALT1) to 25.2% (Phoenix, PHOE1). Light-absorbing carbon was an important contributor to  $b_{\text{ext}}$  for many urban CSN sites in the western United States, specifically. Values ranged from 5.01% (Bonne Terre, Missouri, #291860005) to 36.3% in Nevada (Las Vegas, #320030020) (Figure 3.5d). The spatial gradients in the relative contribution of LAC to  $b_{\text{ext}}$  were somewhat more diffuse than the spatial gradients in  $b_{\text{ext\_LAC}}$ .

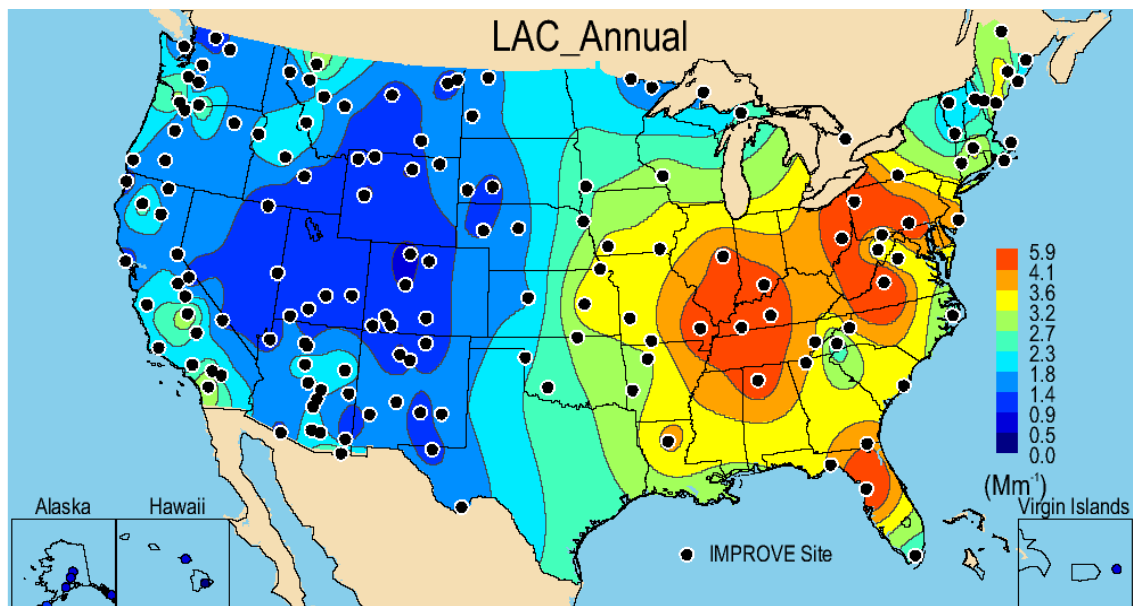


Figure 3.5a.  $\text{PM}_{2.5}$  reconstructed ambient annual mean light extinction coefficient for light absorbing carbon ( $b_{\text{ext\_LAC}}$ ,  $\text{Mm}^{-1}$ ) for 2005–2008 for rural IMPROVE sites. The “modified original” IMPROVE algorithm was used (see text). Wavelength corresponds to 550 nm.

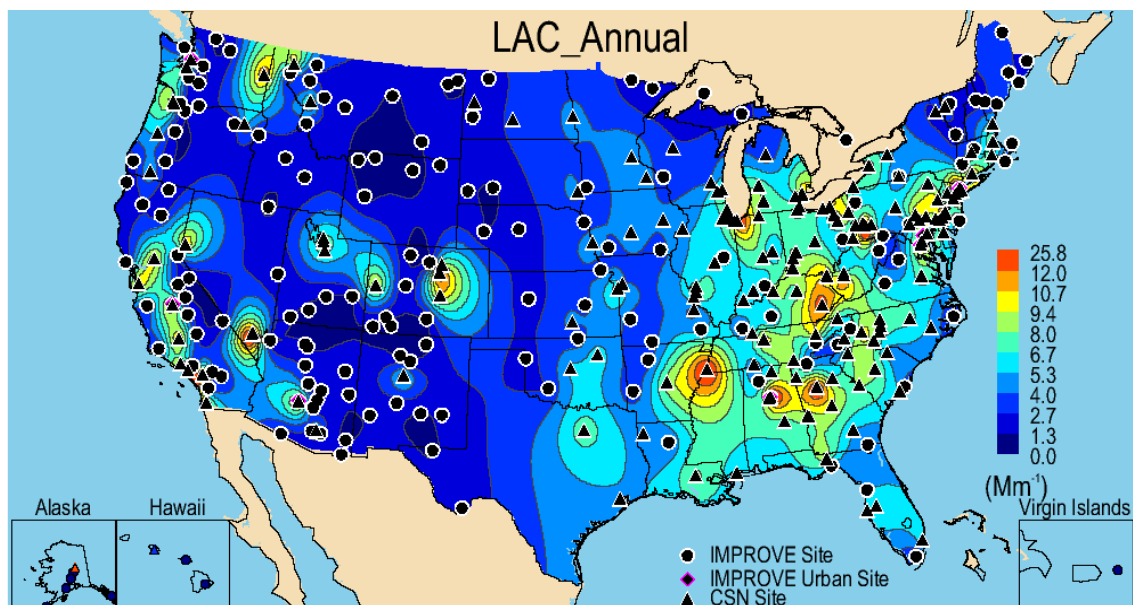


Figure 3.5b.  $\text{PM}_{2.5}$  reconstructed ambient annual mean light extinction coefficient for light absorbing carbon ( $b_{\text{ext,LAC}}$ ,  $\text{Mm}^{-1}$ ) for 2005–2008 for rural IMPROVE and urban CSN sites. The “modified original” IMPROVE algorithm was used (see text). Wavelength corresponds to 550 nm.

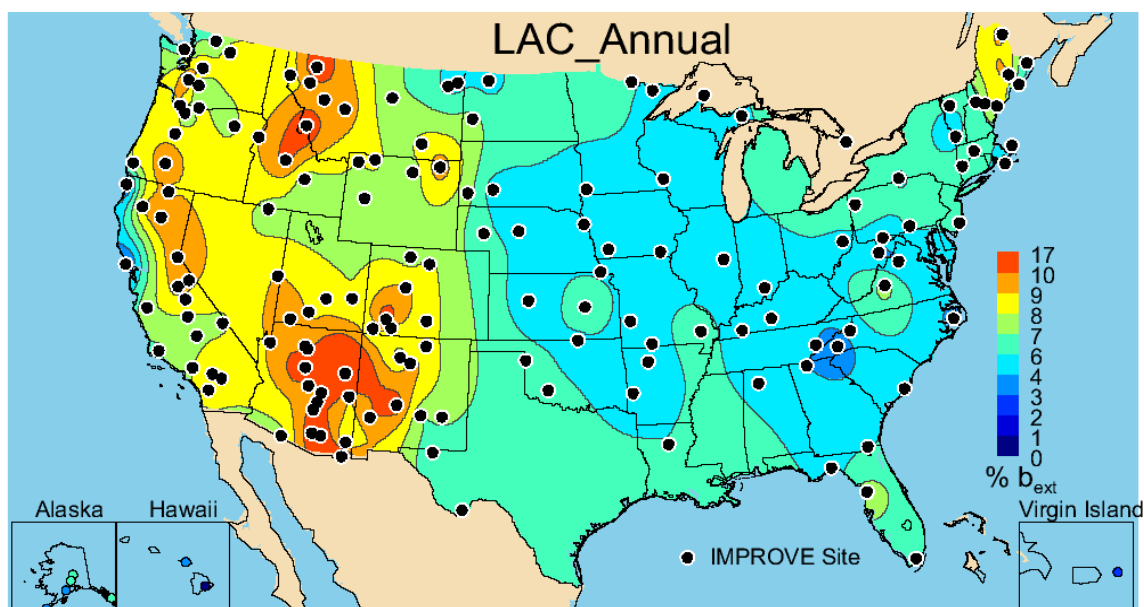


Figure 3.5c. Annual mean percent contribution (%) of ambient light absorbing carbon (LAC) light extinction coefficient ( $b_{\text{ext}}$ ) to  $\text{PM}_{2.5}$  reconstructed aerosol  $b_{\text{ext}}$  for 2005–2008 for rural IMPROVE sites. The “modified original” IMPROVE algorithm was used (see text). Wavelength corresponds to 550 nm.

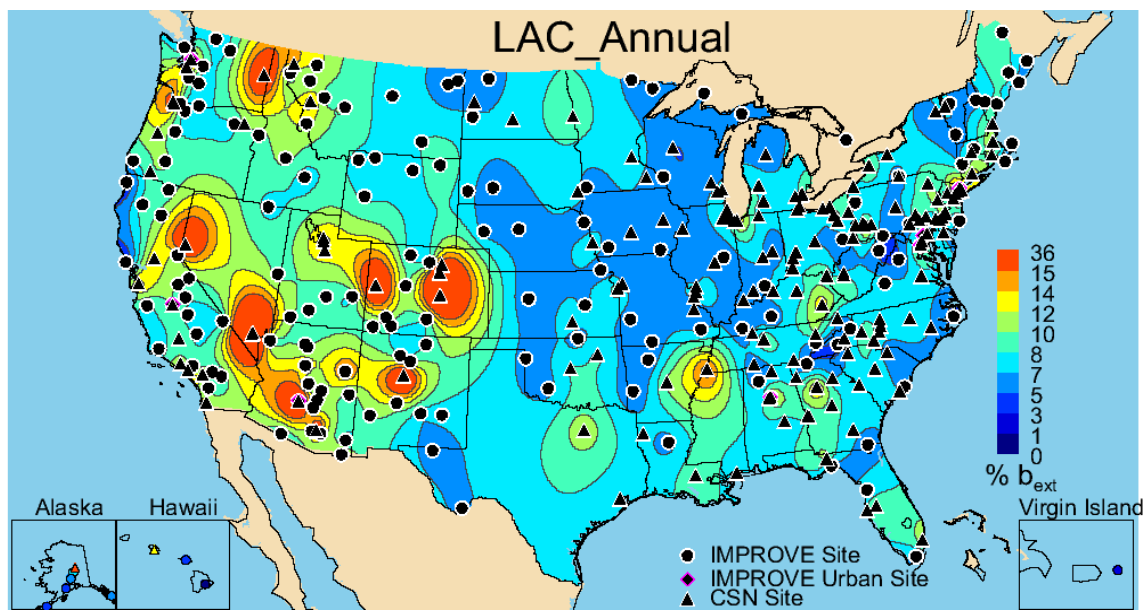


Figure 3.5d. Annual mean percent contribution (%) of ambient light absorbing carbon (LAC) light extinction coefficient ( $b_{ext}$ ) to  $PM_{2.5}$  reconstructed aerosol  $b_{ext}$  for 2005–2008 for rural IMPROVE and urban CSN sites. The “modified original” IMPROVE algorithm was used (see text). Wavelength corresponds to 550 nm.

### 3.6 $PM_{2.5}$ FINE SOIL LIGHT EXTINCTION COEFFICIENTS

The annual mean soil  $b_{ext}$  ( $b_{ext\_soil}$ ) spatial pattern was the same as the fine soil mass concentration pattern (Figure 3.6a). The rural IMPROVE  $b_{ext\_soil}$  ranged from  $0.11 \text{ Mm}^{-1}$  in Petersburg, Alaska (PETE1), to  $4.41 \text{ Mm}^{-1}$  in Douglas, Arizona (DOUG1). The urban IMPROVE  $b_{ext\_soil}$  had a similar range, from  $0.49 \text{ Mm}^{-1}$  in Puget Sound (PUSO1) to  $3.22 \text{ Mm}^{-1}$  in Phoenix (PHOE1). Generally the southern half of the United States had higher  $b_{ext\_soil}$ , but values were relatively low; only ten sites had annual mean  $b_{ext\_soil}$  greater than  $1.5 \text{ Mm}^{-1}$ . The addition of data from CSN sites provided further detail to the spatial pattern of  $b_{ext\_soil}$  (Figure 3.6b) but did not alter it substantially. Sites in Colorado (Denver,  $1.61 \text{ Mm}^{-1}$ , #080010006), Washington (Spokane,  $1.55 \text{ Mm}^{-1}$ , #530630016), and Alabama (Birmingham,  $1.35 \text{ Mm}^{-1}$ , #010730023) had higher  $b_{ext\_soil}$ . Only nine CSN sites had  $b_{ext\_soil}$  greater than  $1.5 \text{ Mm}^{-1}$ .

The largest percent contributions to aerosol  $b_{ext}$  from fine soil at rural IMPROVE sites occurred in the West and Southwest (Figure 3.6c). Percent contributions at rural sites ranged from 0.49% (Simeonof, Alaska, SIME1) to 18.4% in Douglas, Arizona (DOUG1). Soil contributed over 10% to  $b_{ext}$  for only nine sites; with the exception of Jarbidge, Nevada (JARB1), and the Virgin Islands (VIIS1), all of the sites were in Arizona. The urban IMPROVE percent contributions ranged from 0.65% in Baltimore (BALT1) to 7.5% in Phoenix (PHOE1). A similar range was found for the CSN sites, from 0.30% in Arendtsville, Pennsylvania (#420010001), to 5.2% in Las Vegas (#320030020). Soil was not a major contributor to urban CSN  $b_{ext}$  (Figure 3.6d). No CSN sites had contributions greater than 10%.

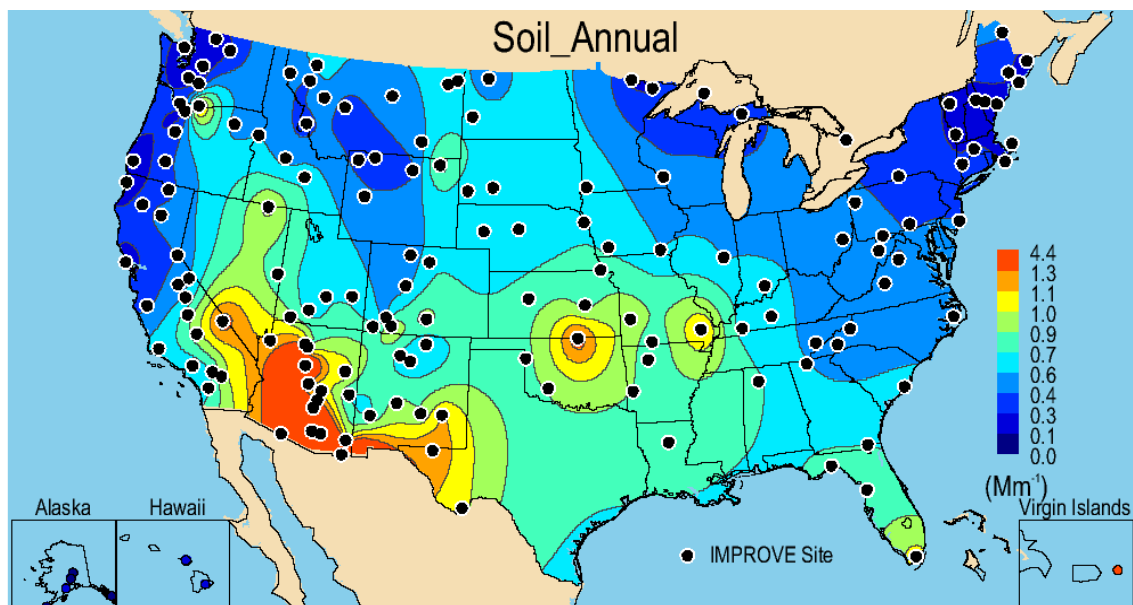


Figure 3.6a.  $PM_{2.5}$  reconstructed ambient annual mean light extinction coefficient for soil ( $b_{ext\_soil}$ ,  $Mm^{-1}$ ) for 2005–2008 for rural IMPROVE sites. The “modified original” IMPROVE algorithm was used (see text). Wavelength corresponds to 550 nm.

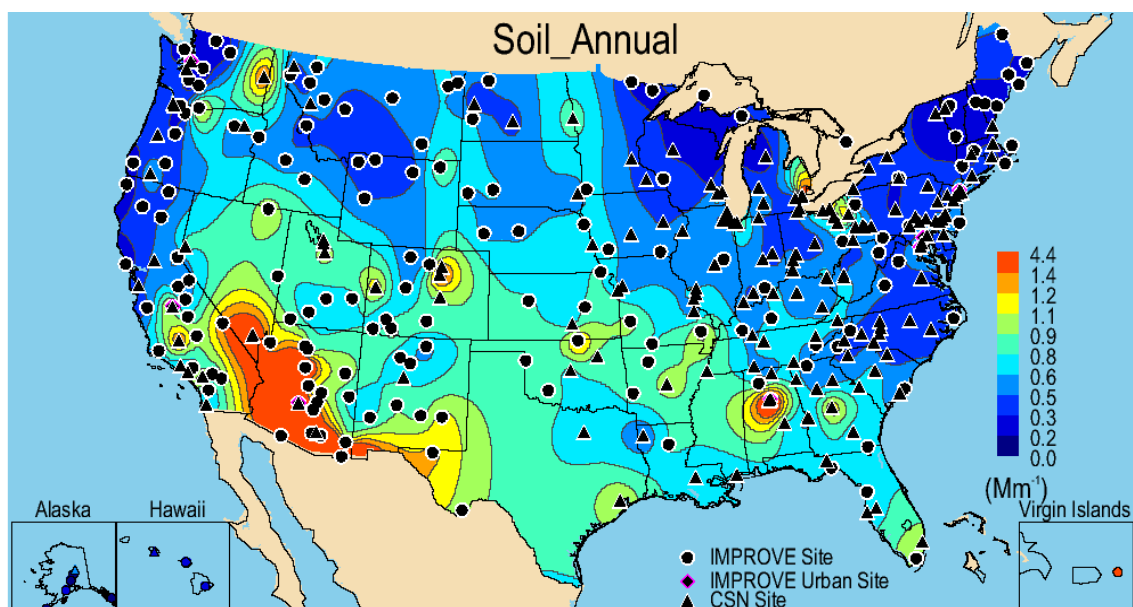


Figure 3.6b.  $PM_{2.5}$  reconstructed ambient annual mean light extinction coefficient for soil ( $b_{ext\_soil}$ ,  $Mm^{-1}$ ) for 2005–2008 for rural IMPROVE and urban CSN sites. The “modified original” IMPROVE algorithm was used (see text). Wavelength corresponds to 550 nm.

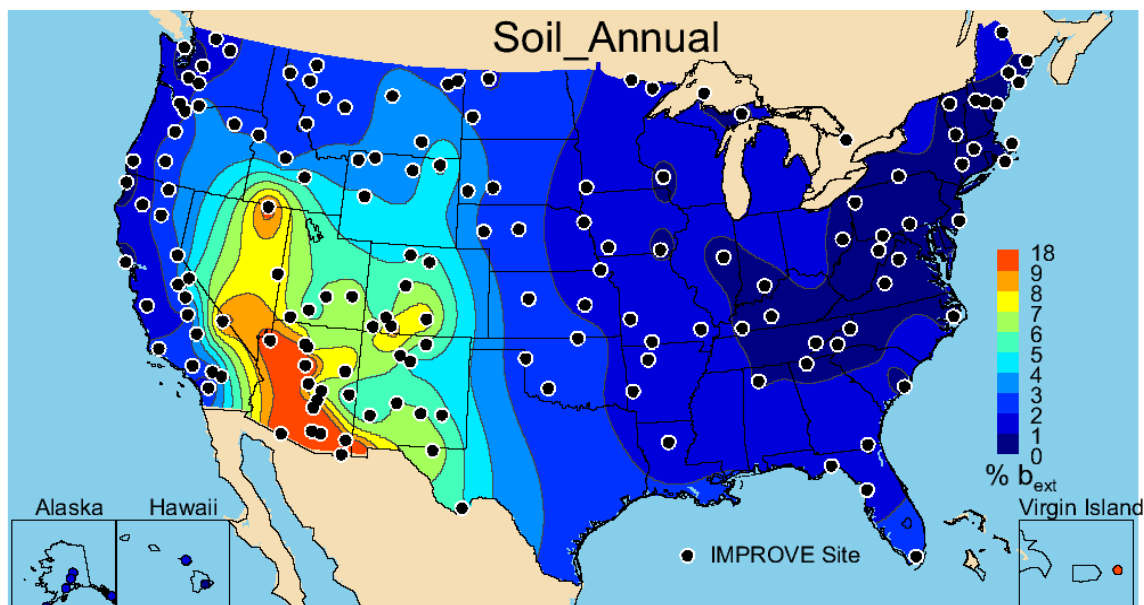


Figure 3.6c. Annual mean percent contribution (%) of ambient soil light extinction coefficient ( $b_{ext}$ ) to  $PM_{2.5}$  reconstructed aerosol  $b_{ext}$  for 2005–2008 for rural IMPROVE sites. The “modified original” IMPROVE algorithm was used (see text). Wavelength corresponds to 550 nm.

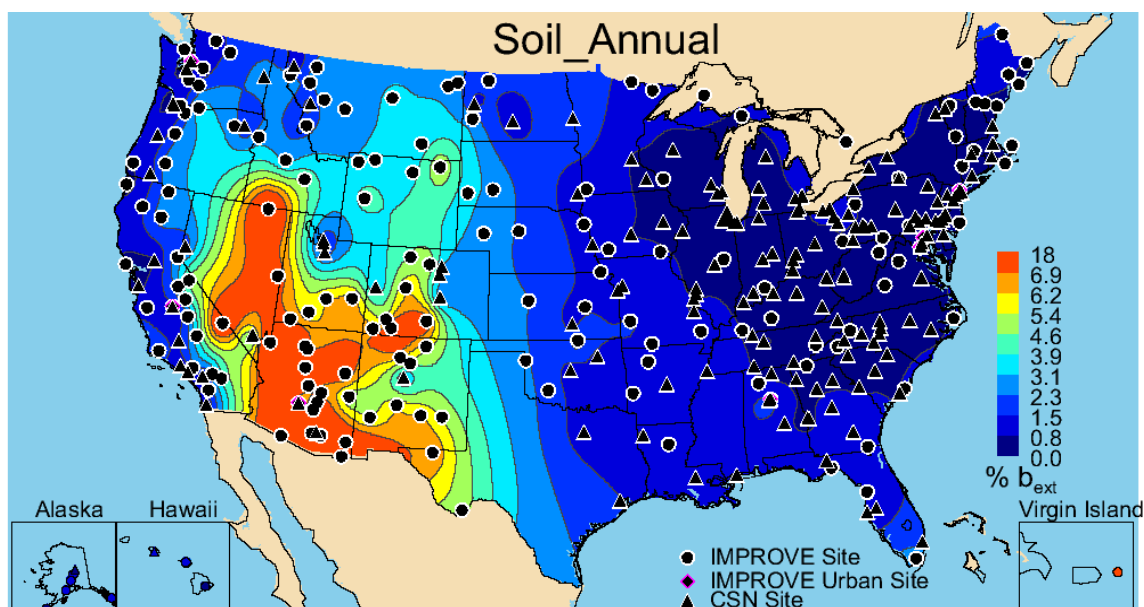


Figure 3.6d. Annual mean percent contribution (%) of ambient soil light extinction coefficient ( $b_{ext}$ ) to  $PM_{2.5}$  reconstructed aerosol  $b_{ext}$  for 2005–2008 for rural IMPROVE and urban CSN sites. The “modified original” IMPROVE algorithm was used (see text). Wavelength corresponds to 550 nm.

### 3.7 $PM_{2.5}$ SEA SALT EXTINCTION COEFFICIENTS

Spatial patterns of IMPROVE 2005–2008 monthly mean light extinction coefficients due to sea salt ( $b_{ext\_SS}$ ) were very similar to sea salt mass concentrations. All IMPROVE values ranged from  $0.04 \text{ Mm}^{-1}$  (Cloud Peak, Wyoming, CLPE1) to  $12.8 \text{ Mm}^{-1}$  (Point Reyes National Seashore, California, PORE1). Generally  $b_{ext\_SS}$  was relatively low; only in coastal regions were estimates non-negligible. Eight sites corresponded to annual mean  $b_{ext\_SS}$  values greater than 3

$\text{Mm}^{-1}$ , and these were located in coastal regions, including the Virgin Islands (VIIS1) (see Figure 3.7a). The coastal pattern of elevated  $b_{\text{ext\_SS}}$  was also observed with the inclusion of CSN sites where only three sites (in Hawaii, Florida, and Pennsylvania) were greater than  $3 \text{ Mm}^{-1}$  (Figure 3.7b). The maximum  $b_{\text{ext\_SS}}$  occurred at Pearl City, Hawaii ( $5.33 \text{ Mm}^{-1}$ , #150032004), and the minimum  $b_{\text{ext\_SS}}$  occurred at Watford City, North Dakota ( $0.0075 \text{ Mm}^{-1}$ , #380530002).

The IMPROVE percent contribution of sea salt to  $b_{\text{ext}}$  was typically low on an annual mean basis, except at coastal sites where the maximum IMPROVE contribution (41.1%) occurred at Simeonof, Alaska (SIME1) (Figure 3.7c). The lowest contribution of SS to  $b_{\text{ext}}$  occurred at Frostberg Reservoir, Maryland (0.29%, FRRE1). Only eighteen sites corresponded to contributions of greater than 5%. The largest percent contribution for CSN occurred at Pearl City, Hawaii (23.0%, #150032004). Besides the Hawaii site, only one other CSN site in Florida had contributions from sea salt to  $b_{\text{ext}}$  greater than 5% (Fort Lauderdale, #120111002) (Figure 3.7d). The lowest percent contribution occurred at Watford City, North Dakota (0.034%, #380530002)

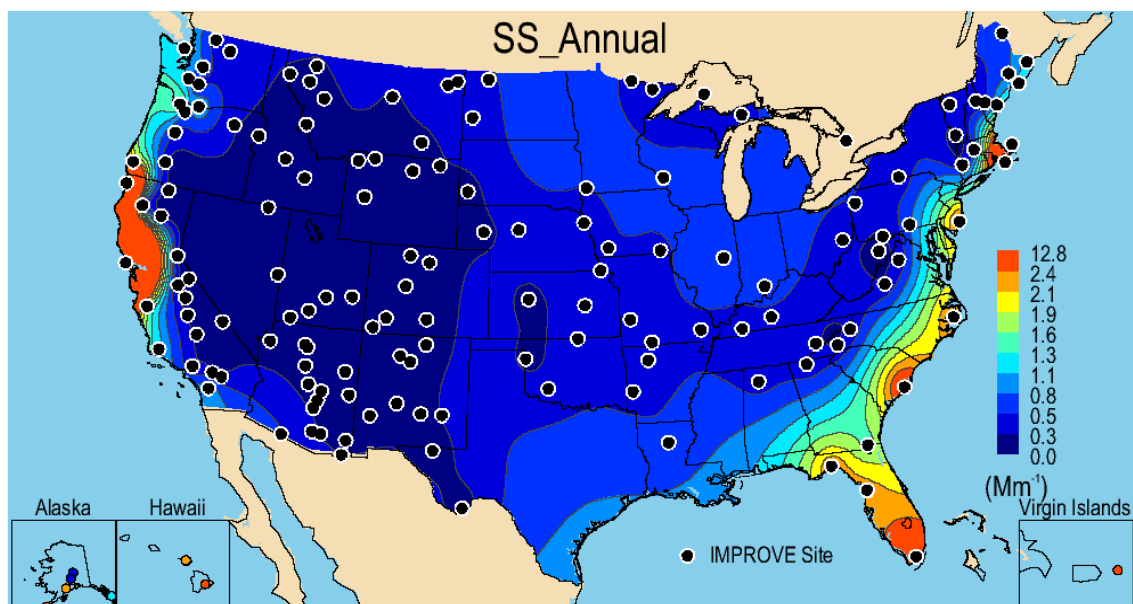


Figure 3.7a.  $\text{PM}_{2.5}$  reconstructed ambient annual mean light extinction coefficient for sea salt ( $b_{\text{ext\_SS}}, \text{Mm}^{-1}$ ) for 2005–2008 for rural IMPROVE sites. The “modified original” IMPROVE algorithm was used (see text). Wavelength corresponds to 550 nm.

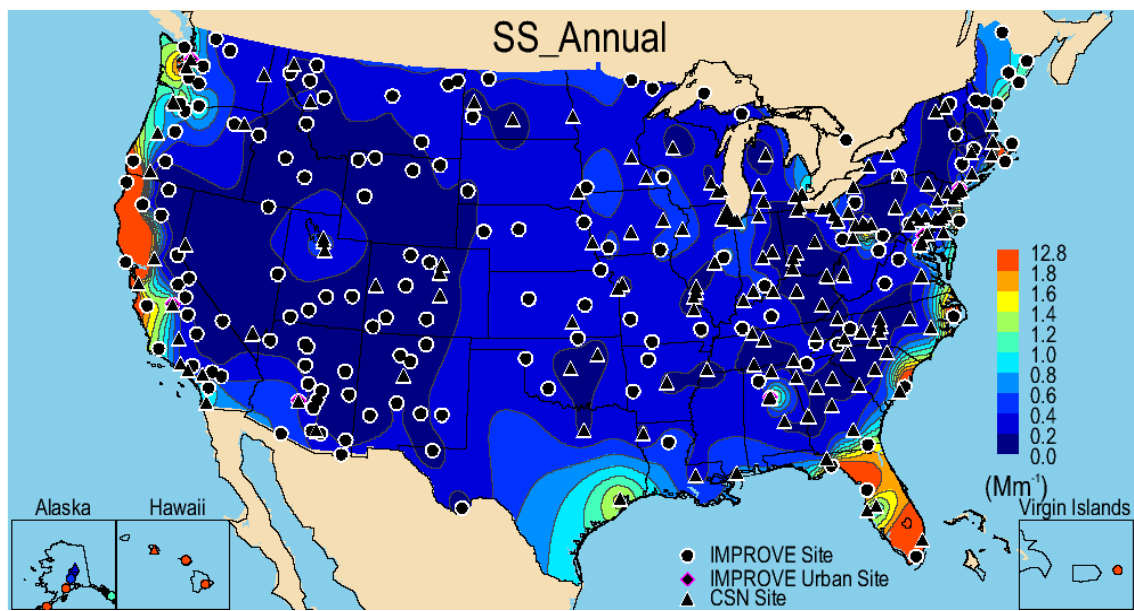


Figure 3.7b.  $PM_{2.5}$  reconstructed ambient annual mean light extinction coefficient for sea salt ( $b_{ext,SS}$ ,  $Mm^{-1}$ ) for 2005–2008 for rural IMPROVE and urban CSN sites. The “modified original” IMPROVE algorithm was used (see text). Wavelength corresponds to 550 nm.

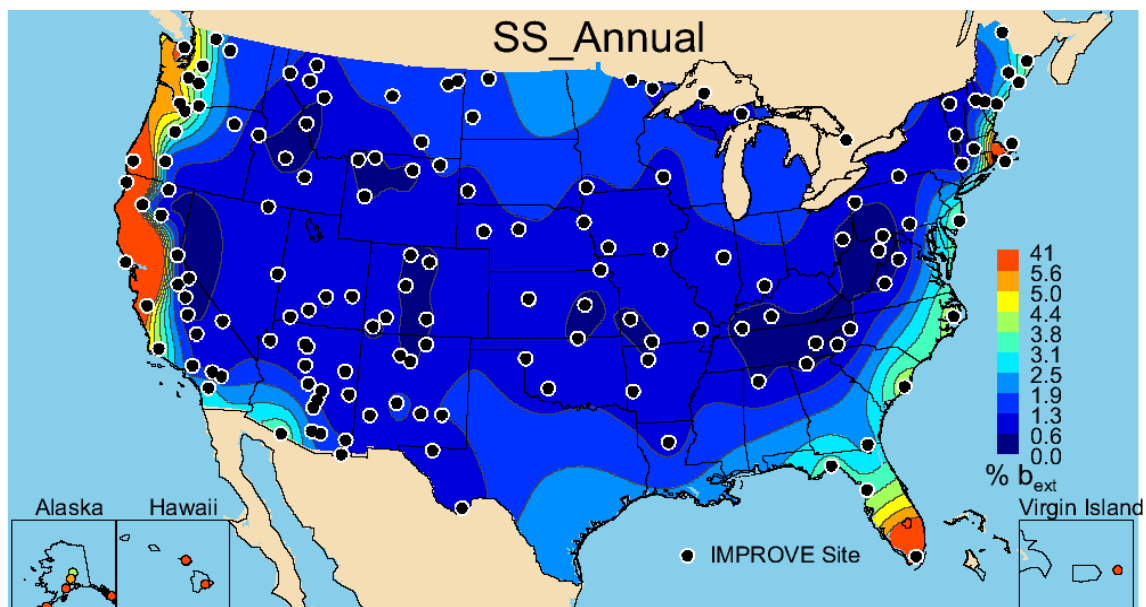


Figure 3.7c. Annual mean percent contribution (%) of ambient sea salt (SS) light extinction coefficient ( $b_{ext}$ ) to  $PM_{2.5}$  reconstructed aerosol  $b_{ext}$  for 2005–2008 for rural IMPROVE sites. The “modified original” IMPROVE algorithm was used (see text). Wavelength corresponds to 550 nm.

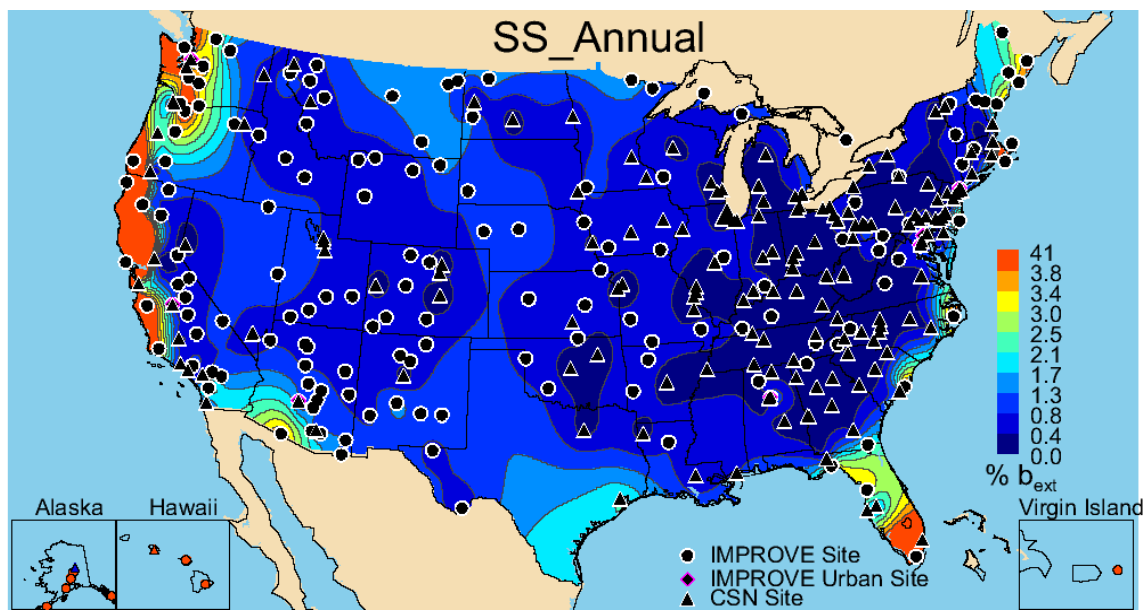


Figure 3.7d. Annual mean percent contribution (%) of ambient sea salt (SS) light extinction coefficient ( $b_{ext}$ ) to  $PM_{2.5}$  reconstructed aerosol  $b_{ext}$  for 2005–2008 for rural IMPROVE and urban CSN sites. The “modified original” IMPROVE algorithm was used (see text). Wavelength corresponds to 550 nm.

### 3.8 $PM_{2.5}$ RECONSTRUCTED AEROSOL LIGHT EXTINCTION COEFFICIENTS

For the purposes of this discussion,  $PM_{2.5}$  aerosol  $b_{ext}$  ( $b_{ext\_aer}$ ) refers to the sum of  $PM_{2.5}$   $b_{ext}$  from ammonium sulfate, ammonium nitrate, particulate organic carbon, light absorbing carbon, fine soil, and sea salt. Rayleigh scattering was not included, and light extinction coefficients due to coarse mass will be investigated separately. The 2005–2008 IMPROVE rural annual mean  $b_{ext}$  is presented in Figure 3.8a. The east-west division observed for several species (especially  $b_{ext\_AS}$ ) was preserved in the aggregation of aerosol  $b_{ext}$ . Generally the highest rural aerosol  $b_{ext}$  occurred in the East and along the Ohio River valley. The values ranged from  $8.24 \text{ Mm}^{-1}$  in Petersburg, Alaska (PETE1), to  $95.54 \text{ Mm}^{-1}$  in Mammoth Cave, Kentucky (MACA1). Recall that the major contributor to  $b_{ext\_aer}$  at this site was ammonium sulfate (68%), and in fact the spatial pattern of  $b_{ext\_aer}$  is similar to  $b_{ext\_AS}$  (compare Figures 3.2a and 3.8a). Urban IMPROVE sites corresponded to higher  $b_{ext\_aer}$  and ranged from  $42.05 \text{ Mm}^{-1}$  in Phoenix (PHOE5) to  $117.65 \text{ Mm}^{-1}$  in Birmingham (BIRM1). The addition of CSN sites enhanced the spatial resolution in the East but did not alter the contrast between  $b_{ext\_aer}$  in the eastern and western United States (Figure 3.8b). Values ranged from  $22.17 \text{ Mm}^{-1}$  in North Dakota (Watford City, #380530002) to  $146.97 \text{ Mm}^{-1}$  in Pennsylvania (Liberty, #420030064). Most CSN sites (92%) corresponded to higher  $b_{ext\_aer}$  ( $>50 \text{ Mm}^{-1}$ ), probably due to their location in the eastern United States, where AS was a dominant contributor to  $b_{ext}$ . On the West Coast, higher urban  $b_{ext\_aer}$  was most likely due to the contribution from ammonium nitrate. Recall that the site in Bakersfield corresponded to a 54% contribution from ammonium nitrate to  $b_{ext}$ .

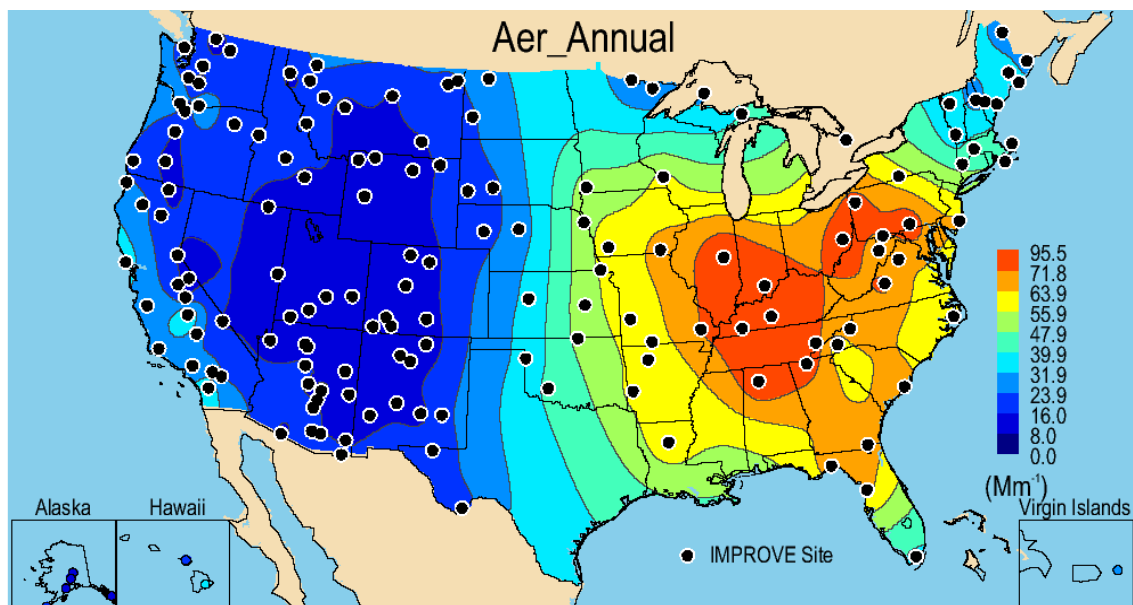


Figure 3.8a.  $PM_{2.5}$  reconstructed annual mean light extinction coefficient for ambient aerosol ( $b_{ext\_aer}$ ,  $Mm^{-1}$ ) for 2005–2008 for rural IMPROVE sites. The “modified original” IMPROVE algorithm was used (see text). Wavelength corresponds to 550 nm.

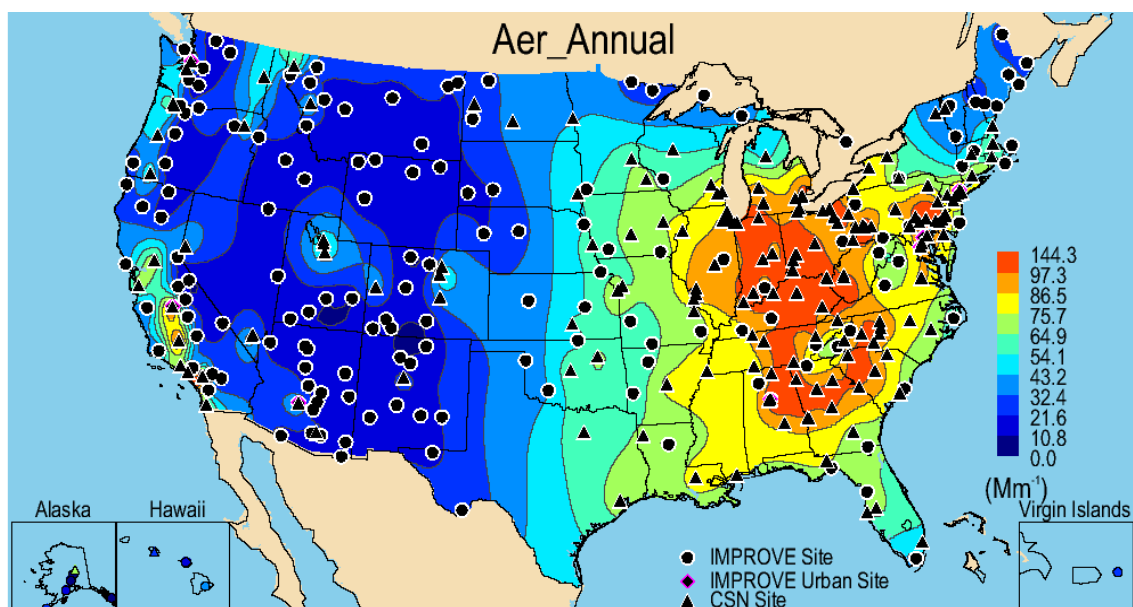


Figure 3.8b.  $PM_{2.5}$  reconstructed annual mean light extinction coefficient for ambient aerosol ( $b_{ext\_aer}$ ,  $Mm^{-1}$ ) for 2005–2008 for rural IMPROVE and urban CSN sites. The “modified original” IMPROVE algorithm was used (see text). Wavelength corresponds to 550 nm.

### 3.9 COARSE MASS LIGHT EXTINCTION COEFFICIENTS

Although coarse mass was not included in aerosol  $b_{ext}$  because it is not measured by the CSN network, we computed light extinction coefficients due to coarse mass ( $b_{ext\_CM}$ ) separately for IMPROVE sites. The spatial pattern of  $b_{ext\_CM}$  reflected the pattern of the coarse mass concentration distribution (Figure 3.9a). Urban and rural IMPROVE  $b_{ext\_CM}$  had similar ranges, with the highest nearing that of Rayleigh scattering contributions. The overall maximum

occurred at Douglas, Arizona ( $12.67 \text{ Mm}^{-1}$ , DOUG1), and was most likely associated with soil, as the maximum  $b_{\text{ext\_soil}}$  was also computed for this site. The lowest  $b_{\text{ext\_CM}}$  occurred at North Cascades, Washington ( $0.68 \text{ Mm}^{-1}$ , NOCA1). Regions in the Midwest and Southwest and urban locations in Birmingham ( $9.37 \text{ Mm}^{-1}$ , BIRM1) and Fresno ( $11.89 \text{ Mm}^{-1}$  FRES1) corresponded to higher  $b_{\text{ext\_CM}}$ . In fact, of the four sites with  $b_{\text{ext\_CM}}$  values greater than  $10 \text{ Mm}^{-1}$ , three of them were urban (Douglas, Arizona; Fresno; and two sites in Phoenix, PHOE1 and PHOE5), which were not included in the map of rural  $b_{\text{ext\_CM}}$  shown in Figure 3.9a. Similar to the discussion of CM mass concentration, elevated  $b_{\text{ext\_CM}}$  occurred at several sites in the Midwest and mid-South. High  $b_{\text{ext\_soil}}$  did not coincide with these site locations, suggesting other CM species were contributing to  $b_{\text{ext}}$  at these sites. Many IMPROVE sites corresponded to low  $b_{\text{ext\_CM}}$ ; 39% of IMPROVE sites had  $b_{\text{ext\_CM}}$  less than  $2 \text{ Mm}^{-1}$ .

The annual mean IMPROVE fractional contributions of  $b_{\text{ext\_CM}}$  to total aerosol  $b_{\text{ext}}$  were computed separately from the species discussed above; for this case, total  $b_{\text{ext}}$  included the contribution from coarse mass. Fractional contributions of  $b_{\text{ext\_CM}}$  ranged from 2.2% at Shining Rock Wilderness, North Carolina (SHRO1) to 34.5% in Douglas, Arizona (DOUG1) (see Figure 3.9b). The contributions of CM to  $b_{\text{ext}}$  were most important at the Intermountain West and Southwest, where CM contributed 20% or more to total  $b_{\text{ext}}$ . In the Intermountain West, light extinction due to other species was of similar magnitude to coarse mass  $b_{\text{ext}}$ , resulting in contributions of  $b_{\text{ext\_CM}}$  to total  $b_{\text{ext}}$  that were non-negligible. While annual mean  $b_{\text{ext\_CM}}$  was higher in the Central and Midwest regions compared to the Intermountain West region, its contribution to total  $b_{\text{ext}}$  was not as important, largely due to the relatively higher contributions of ammonium nitrate to  $b_{\text{ext}}$  in the Midwest. The contribution of CM to  $b_{\text{ext}}$  was even less important in the eastern United States, where contributions were typically less than 10%.

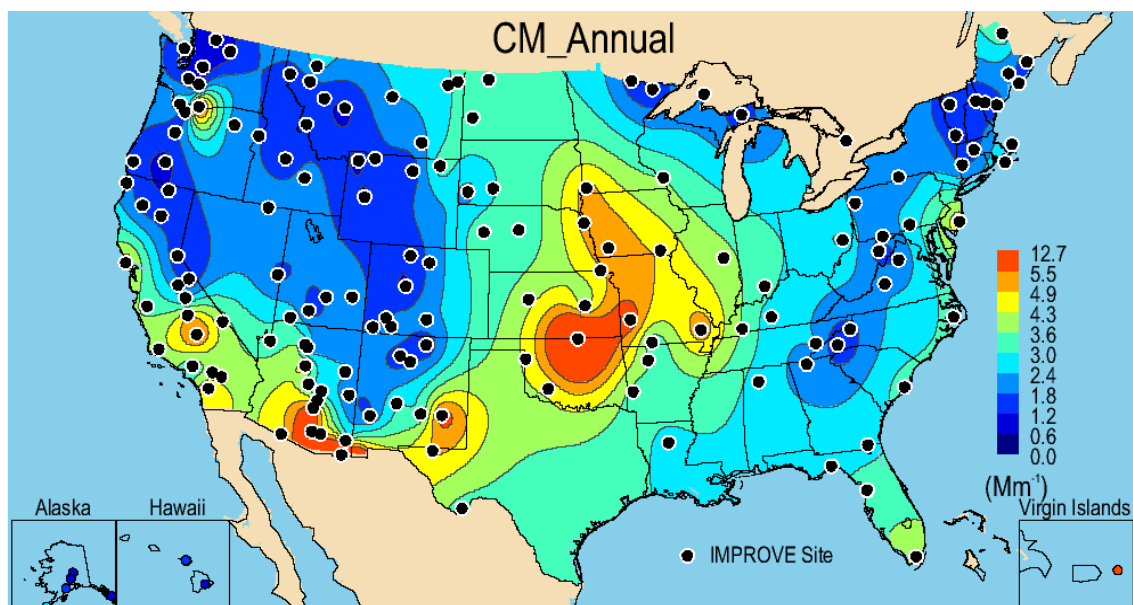


Figure 3.9a. Annual mean light extinction coefficient for coarse mass ( $b_{\text{ext\_CM}}$ ,  $\text{Mm}^{-1}$ ) for 2005–2008 for rural IMPROVE sites. The “modified original” IMPROVE algorithm was used (see text). Wavelength corresponds to 550 nm.

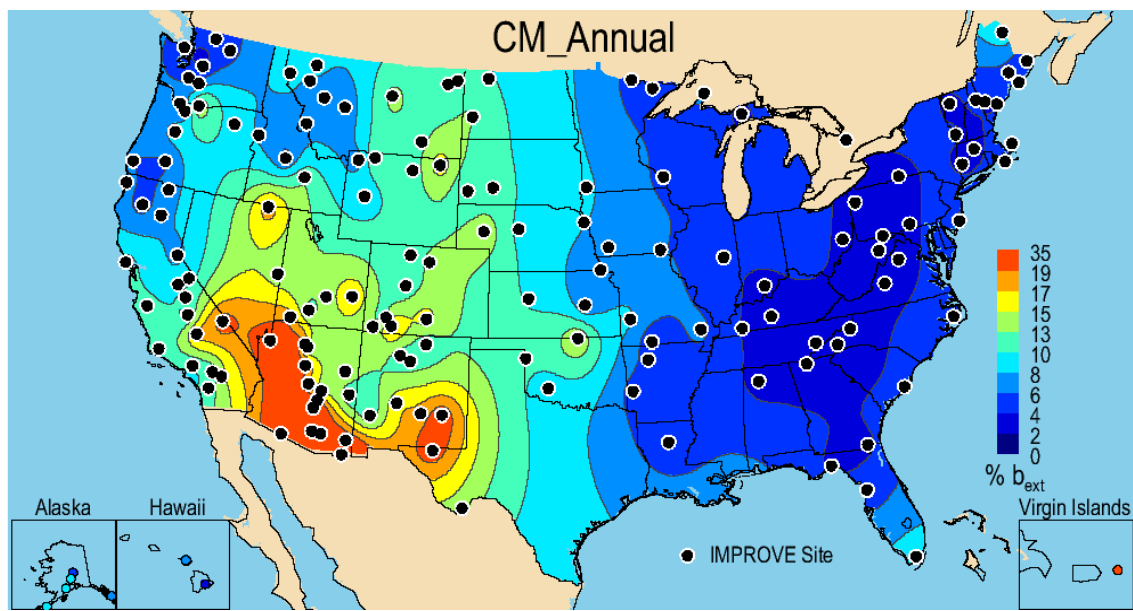


Figure 3.9b. Annual mean percent contribution (%) of coarse mass (CM) light extinction coefficient to total reconstructed aerosol  $b_{ext}$  for 2005–2008 for rural IMPROVE sites. The “modified original” IMPROVE algorithm was used (see text). Wavelength corresponds to 550 nm. Rayleigh scattering was not included in total  $b_{ext}$ .

### 3.10 PM<sub>2.5</sub> DECIVIEW

The 2005–2008 IMPROVE annual mean deciview (dv) spatial pattern was very similar to the  $b_{ext\_aer}$  pattern, as expected (see Figure 3.10). The main differences were that the contributions of coarse mass and site-specific Rayleigh scattering were included (see equation 3.5). Higher dv values were observed in the eastern United States. Values at rural sites ranged from 4.65 dv at White River NF, Colorado (WHRI1), to 22.19 dv at Mammoth Cave, Kentucky (MACA1). Urban IMPROVE sites corresponded to a similar range, with 17.04 dv in Phoenix (PHOE1) to 24.13 dv in Birmingham (BIRM1). No interpolated map of dv with CSN data was produced because coarse mass data are not available from the CSN network.

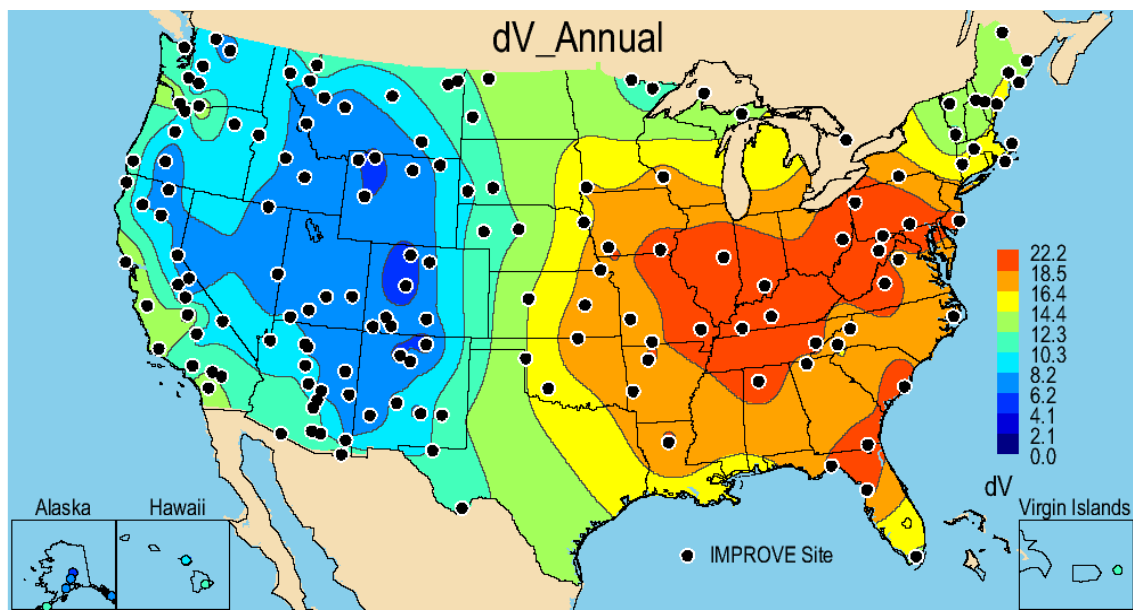


Figure 3.10. Annual mean PM<sub>2.5</sub> deciview (dv) for 2005–2008 for rural IMPROVE sites. The “modified” IMPROVE algorithm was used (see text). Wavelength corresponds to 550 nm.

Tables of the 2005–2008 annual mean  $b_{\text{ext}}$  and  $b_{\text{ext}}$  fractions are reported for each site in Appendix C.1 (IMPROVE and CSN  $b_{\text{ext}}$ ) and C.2 (IMPROVE and CSN relative  $b_{\text{ext}}$ ).

## REFERENCES

- Brewer, P., and T. Moore (2009), Source contributions to visibility impairment in the southeastern and western United States, *J. Air & Waste Manage. Assoc.*, *59*, 1070-1081, doi:10.3155/1047-3289.59.9.1070.
- Hand, J. L., and W. C. Malm (2006), Review of the IMPROVE equation for estimating ambient light extinction coefficients, CIRA Report, ISSN: 0737-5352-71, Colo. State Univ., Fort Collins.
- Hand, J. L., and W. C. Malm (2007), Review of aerosol mass scattering efficiencies from ground-based measurements since 1990, *J. Geophys. Res.*, *112*, D16203, doi:10.1029/2007JD008484.
- Hand, J. L., D. E. Day, G. R. McMeeking, E. J. T. Levin, C. M. Carrico, S. M. Kreidenweis, W. C. Malm, A. Laskin, and Y. Desyaterik (2010), Measured and modeled humidification factors of fresh smoke particles from biomass burning: role of inorganic constituents, *Atmos. Chem. Phys.*, *10*, 6179-6194, doi:10.5194/acp-10-6179-2010.
- Lowenthal, D. H., and N. Kumar (2003), PM<sub>2.5</sub> mass and light extinction reconstruction in IMPROVE, *J. Air & Waste Manage. Assoc.*, *53*, 1109-1120.
- Malm, W. C., J. F. Sisler, D. Huffman, R. A. Eldred, and T. A. Cahill (1994), Spatial and seasonal trends in particle concentration and optical extinction in the United States, *J. Geophys. Res.*, *99(D1)*, 1347-1370.

- Malm, W. C., D. E. Day, C. Carrico, S. M. Kreidenweis, J. L. Collett, Jr., G. McMeeking, T. Lee, J. Carrillo, and B. Schichtel (2005), Intercomparison and closure calculations using measurements of aerosol species and optical properties during the Yosemite Aerosol Characterization Study, *J. Geophys. Res.*, *110*, D14302, doi:10.1029/2004JD005494.
- Malm, W. C., and J. L. Hand (2007), An examination of the physical and optical properties of aerosols collected in the IMPROVE program, *Atmos. Environ.*, *41*, 3407-3427.
- Pitchford, M. L., and W. C. Malm (1994), Development and applications of a standard visual index, *Atmos. Environ.*, *28*, 5, 1049-1054.
- Pitchford, M., W. Malm, B. Schichtel, N. Kumar, D. Lowenthal and J. Hand (2007), Revised algorithm for estimating light extinction from IMPROVE particle speciation data, *J. Air & Waste Manage. Assoc.*, *57*, 1326-1336.
- U. S. EPA (2001), Interpolating relative humidity weighting factors to calculate visibility impairment and the effects of IMPROVE monitor outliers, (<http://vista.cira.colostate.edu/improve/Publications/GuidanceDocs/DraftReportSept20.pdf>).
- U.S. EPA (2003), Draft guidance for tracking progress under the Regional Haze Rule, Contract No. 68-D-02-0261, Work Order No. 1-06, ([http://www.epa.gov/ttn/oarpg/t1/memoranda/rh\\_tpurhr\\_gd.pdf](http://www.epa.gov/ttn/oarpg/t1/memoranda/rh_tpurhr_gd.pdf)).